REGULARIZING INVERSE PROBLEMS

A Dissertation

by

FANG WANG

Submitted to the Office of Graduate and Professional Studies of
Texas A&M University
in partial fulfillment of the requirements for the degree of

DOCTOR OF PHILOSOPHY

Chair of Committee,	Wolfgang Bangerth
Committee Members,	Andrea Bonito
	Yalchin Efendiev
	Jean C. Ragusa
Head of Department,	Emil Straube

August 2014

Major Subject: Department of Mathematics

Copyright 2014 Fang Wang

ABSTRACT

An inverse problem reconstructs the unknown internal parameters of a subject based on collected data derived synthetically or from real measurements. Inverse problems often lack the well-posedness defined by J. Hadamard; in other words, solutions of inverse problems, namely the reconstructions of the parameters, may not exist, may not be unique or may be unstable. Regularization is a technique that deals with such situations.

The well-known Tikhonov regularization method translates the original inverse problem to optimization problems of minimizing the norm of the data misfit plus a weighted regularization functional that incorporates the *a priori* information we may have about the original problem. The choices of the regularization functional $r(q)$ include $\|q\|^2_{L^2}$, $\|q\|^2_{H^1}$, $|q|_{BV}$ and $|q|_{TV}$. However, each of these has its limitations.

In this work, we develop a novel H^s seminorm regularization method and present numerical results for model problems. This method relies on the evaluation of the seminorms of an intermediary Hilbert space, namely H^s space, that stays between L^2 and H^1. The H^s seminorm regularization is designed to minimize the undesirable aspects of the existing L^2 and H^1 regularization functionals. The H^s seminorm regularization also allows discontinuities and stabilizes the perturbations.

We study the H^s seminorm regularization method both theoretically and numerically. We consider the theoretical analysis of this new regularization method based on a model problem. We show that a stable solution can be achieved with some conditions. In addition, we prove the convergence and guarantee a convergence rate provided additional conditions for the model problem when the considered domain is 1D. Numerically, we produce an approximated discretization of the H^s seminorm

regularization that can be applied to 1D, 2D or 3D examples. We also provide reconstructions of both continuous and discontinuous parameters from synthetic data and a comparison of these solutions to the ones based on existing L^2 and H^1 regularization methods. Furthermore, we also apply the H^s seminorm regularization method to a fluorescence optical tomography problem.

In summary, we study and implement the H^s seminorm regularization method for inverse problems, which can provide a stable solution to the model problem. The numerical results indicate the robustness of the new method and suggests that the H^s seminorm regularization method produces the closest approximation of the exact solution than the L^2 norm and H^1 seminorm regularization methods for the model problem.

ACKNOWLEDGEMENTS

I would like to express my sincere gratitude to my advisor, Dr. Wolfgang Bangerth. His inspiration and encouragement have been a consistent guidance, both from a mathematical and human perspective. It was only through his advice that I was able to achieve my goals throughout this research.

I would also like to thank my committee members, Dr. Andrea Bonito, Dr. Yalchin Efendiev and Dr. Jean C. Ragusa, for their guidance and support. I am very grateful for the discussions with Dr. Bangti Jin and Jiayin Liu, which enhanced and benefited my research. I am greatly thankful to Ms Diana Garrison for her carefully editing and proofreading this dissertation, as well as her valuable advice.

My sincere thanks to the rest of the faculty and staff in the mathematics department, as well as my colleagues and friends for their help and support during my graduate years. I thank my family for their understanding and encouragement.

Part of the work presented herein was supported by Award No. KUS-C1-016-04, made by King Abdullah University of Science and Technology (KAUST).

TABLE OF CONTENTS

LIST OF FIGURES

FIGURE Page

1. INTRODUCTION

A problem is "something that is difficult to handle or understand, something that may be a source of trouble or worry", based on the Merriam-Webster Online Dictionary. In mathematics, a problem is "a complicated, unsettled question for consideration or solution", according to the definition on Merriam-Webster Online Dictionary. There are plentiful mathematical problems in general and this piece of work is focused on a selected few called inverse problems.

An inverse problem is one that involves obtaining unknown internal parameters based on information collected by observations. There are many situations where parameters cannot be measured directly, but we may be able to measure some other quantities related to those parameters. For instance, we may consider the sub-surface structure of the Earth without direct measurements available. Once we have the measurement data and know how this data is related to the parameters, the solution involves reconstructing parameters using these facts.

The connection between a normal "forward" problem and an inverse problem is as follows: a "forward" problem requires us to solve for a system's reactions given a complete set of internal parameters and external forces, while an inverse problem conversely involves revealing internal parameters based on given external forces and the system's measured reactions to these forces. Typically, the internal parameters of an inverse problem cannot be measured directly. The solution of inverse problems is, therefore, a description of the previously unknown internal parameters.

Let us consider all the inverse problems, both linear and nonlinear, in a general form:

$$F(q) = z^{\delta} \tag{1.1}$$

where $q \in X$ and $z \in Y$ specify unknown internal parameters and measurement data, respectively (see, e.g. [21]). Here $F : X \to Y$ is an operator between X and Y, where X and Y are Hilbert spaces, or more generally, Banach spaces. The operator F can be linear or nonlinear, which applies to underlying relationships and translates parameters to observation/measurement data. We assume that F takes into account external forcing as well. The measurement data z^δ is a combination of exact data and some level of noise. In order to solve (1.1), an optimization problem minimizes the original problem via the following equation:

$$J(q) := m(q, z^\delta), \tag{1.2}$$

where $m(q, z^\delta)$ is a measurement of the distance between $F(q)$ and z^δ (see, e.g. [6]).

In the next few paragraphs, examples and applications in science and engineering are provided to further explain the concepts of inverse problems, where (1.1) serves as a proxy.

The first example involves two of Earth's parameters; real gravitational acceleration and air friction. These parameters can be estimated by designing an experiment to measure the time and distance of a falling body [3]. In this example, gravitational acceleration and air friction are unknown parameters (q in (1.1)), while time and distance of a falling body are measurement data (observations, z^δ in (1.1)). Their relationship is explained by Newton's second law of motion along with a description of the forces acting on the body. In this example, F in (1.1) represents a map from gravitational acceleration and air friction to time and distance of a falling body.

Another famous example of inverse problems refers to Fredholm integral equations of the first kind:

$$\int_a^b K(x, y) f(y)\, dy = g(x), \tag{1.3}$$

where f is the unknown parameter (q in (1.1)), the kernel function K and the function g on the right-hand side are given measurement data in the problem (z^δ in (1.1)). The kernel K often arises from underlying mathematical models, whereas g typically arises from measurements [27,28]. F in (1.1) in this example transforms f to g as a result of Fredholm integral equations of the first kind.

Using a third example, in the subject of geoscience and petroleum engineering, inverse problems play an important role in detecting the underground structure and hydrogeological properties (q in (1.1)) using seismic waves. A typical procedure is to generate acoustic sources that send out seismic waves, collect the measurement data from a number of receivers in different locations (z^δ in (1.1)), and then solve the problem of determining the geophysical structure of the underground, e.g. the wave speed of the rock (see [34,41,44,50]). F in (1.1) in this example shows a map from the geophysical structure of the underground to collected measurement data.

An important concept of inverse problems is "well-posedness". In general, a problem is said to be well-posed if it satisfies three properties given by J. Hadamard [26]:

1. there exists a solution,
2. the solution is unique, and
3. the solution depends continuously on the input data, a property also called stability.

A problem is ill-posed if it does not satisfy any of these three properties.

Inverse problems are often ill-posed. That is to say, they may not have any solution at all. If there is a solution, it may not be unique. More influentially, a solution to an inverse problem often lacks stability: small changes or perturbations in measurement data can result in large differences in the corresponding solutions – the reconstructed parameters. All these difficulties make solution procedures intricate, both theoretically and practically. However, useful techniques of regularization have been developed and can be applied to counter such problems. Since the original inverse problem is ill-posed, these techniques regularize the problem to a certain solvable extent. The overall goals for regularization are to reduce the ill-posedness of inverse problems, alleviating and mitigating undesirable aspects in the process of identifying a solution.

To regularize a problem, *a priori* information such as boundedness or smoothness is introduced here with the original inverse problem. Tikhonov regularization [25,57], the best-known and most widely-used regularization technique, translates (1.1) to an optimization problem of minimizing the following functional by adding a weighted evaluation of the *a priori* information to the original optimization problem:

$$J_\beta(q) := m(q, z^\delta) + \beta r(q), \tag{1.4}$$

where $m(q, z^\delta)$ is also called the data misfit. The regularization term $\beta r(q)$ consists of two parts: a constant β and a functional $r(q)$ that contains *a priori* information of q (see also [6]).

Some choices for the data misfit $m(q, z^\delta)$ are $\|F(q) - z^\delta\|_{L^2}^2$ [57] and $\|F(q) - z^\delta\|_{L^1}^2$ [16, 30], while choices for the regularization functional $r(q)$ are $\|q\|_{L^2}^2$, $\|q\|_{H^1}^2$ [57], $\|q\|_{BV}$ [1, 49] and $|q|_{TV}$ [14, 15]. The regularization parameter $\beta \in \mathbb{R}_0^+$ balances between the data misfit and the regularization functional. The problem may still be ill-posed if β is too small for the regularization to play its role. However, if β is too large, then the regularization functional dominates and the problem becomes minimizing the regularization, whereas a solution as close as possible to the measurement was originally desired. In general, it is difficult to find the optimal regularization parameter [31].

Using this information, the standard procedure of solving an inverse problem is:

1. making an initial guess of the parameter q,
2. solving for an approximated measurement u of z^δ (also called state) using the relationship between z^δ and q,
3. comparing the result u with the measurement z^δ,
4. updating the current guess for the parameter q, and
5. repeating the last three steps until a desired precision is achieved.

An example of a problem utilizing this general procedure follows:

Nondestructive evaluation is a technique to determine properties of a target without jeopardizing its features. A deflection problem, a category of nondestructive evaluation problems, targets elastic properties such as stiffness. Suppose we would like to detect elastic properties of a body, such as a bar that is one-dimensional (1D) or a membrane that is two-dimensional (2D). The most direct approach of measuring stiffness is to take the target apart and measure it piece by piece. However, breaking a target into parts may not be preferable for reasons such as cost and time consumption; measuring stiffness as an inverse problem can save both. Certain forces can be cast upon the target and we can then measure the corresponding deflection. In this case, however, the natural state of the membrane and the internal relationship between the stiffness and the deflection of the target, which in the current content is a partial differential equation (PDE), must be known.

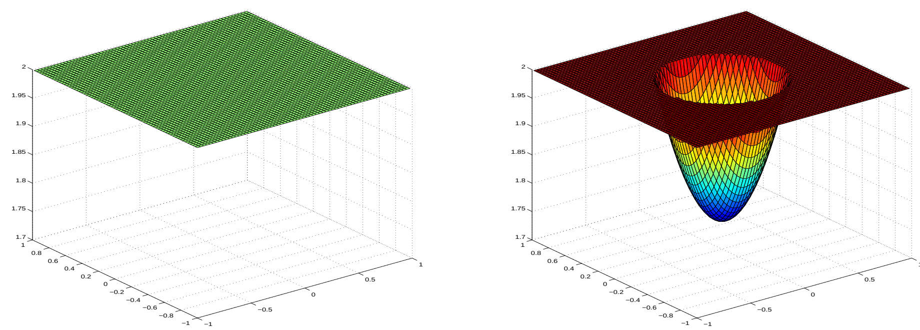

Figure 1.1: The membrane with and without the force application. Left: The rest state of the membrane. Right: The deflected membrane under force $f(x)$.

A mathematical formulation is sketched as follows: for the target membrane, the deflection $u(x)$ is subject to a Poisson equation:

$$-\nabla \cdot q(x)\nabla u(x) = f(x), \tag{1.5}$$

where $f(x)$ is the given force and $q(x)$ is the stiffness of the membrane we seek. Here $q(x)$ is bounded almost everywhere, namely there exist constants c_0 and c_1 such that $c_0 \le q(x) \le c_1$ almost everywhere. Suitable boundary conditions need also be applied. Applying (1.1), the general form for this particular problem is:

$$F(q) := u_q. \tag{1.6}$$

Assume that the measurement of the deflection under a given force can be made anywhere in Ω denoted by z^δ. The predicted deflection $u_q(x)$ can be found by solving the PDE (1.5). Therefore, our purpose is to find such a $q(x)$ that $u_q(x)$ would match z^δ best under certain criteria. The typical least squares method minimizes the residual (called data misfit) (1.2), whose mathematical setting is:

$$\begin{aligned}&\min_{u,q} J(q) := m(q, z^\delta),\\ &\text{subject to} \quad -\nabla \cdot q(x)\nabla u(x) = f(x),\end{aligned}$$

where $m(q, z^\delta)$ evaluates the distance between $F(q)$ and z^δ.

As mentioned before, since inverse problems are typically ill-posed, we introduce Tikhonov regularization, which adds a weighted term to the original optimization problem. Thus, the formula after adding Tikhonov regularization becomes (see also [6]):

$$\begin{aligned}&\min_{u,q} J_\beta(q) := m(q, z^\delta) + \beta r(q),\\ &\text{subject to} \quad -\nabla \cdot q(x)\nabla u(x) = f(x).\end{aligned} \tag{1.7}$$

This β balances the data misfit and regularization (see [17] for example), whereas $r(q)$ consists of *a priori* information of q. Frequent choices for this functional $r(q)$ are $\|q\|^2_{L^2}$, $\|q\|^2_{H^1}$, $|q|_{BV}$ and $|q|_{TV}$. However, each of these has its limitations. The L^2 norm minimizes the parameter itself but does not make any assumption about the smoothness of the parameter $q(x)$; consequently, oscillations will not be suppressed. On the other hand, the H^1 norm takes into account the parameter along with the first order derivative of the parameter. Nevertheless, minimizing the H^1 norm would make the solution too smooth because it minimizes the derivative as well, discarding all the jumps. Total variations are good regularization criteria because they allow discontinuous functions, yet limit the size of the jump. However, they are not quadratic norms and not differentiable, which makes them difficult to solve in the numerical steps, especially when using Newton's method.

Choosing a proper norm for the regularization functional is challenging because of the number of aspects to resolve. Consequently, a new regularization criterion, the H^s seminorm regularization, is introduced here. H^s spaces lie between L^2 and H^1. Resulting from the definition of H^s spaces, the H^s seminorm regularization is designed to minimize the undesirable aspects of the existing L^2 and H^1 regularization functionals. Ideally, H^s seminorm regularization will mimic the discontinuities and stabilize the perturbations.

The second section deals with the theoretical analysis of this newly-developed regularization method. Concise mathematical definitions of H^s spaces and H^s seminorms are introduced. Along with necessary preliminary definitions and theorems, the main topic in this section is to demonstrate the existence and stability of the nondestructive model problem using the H^s seminorm regularization method.

The third and fourth sections discuss the study of computational reconstruction approaches using this regularization. In the third section, the general scheme of numerical solutions and in particular, a H^s seminorm discretization are the major subjects. In the fourth section, concrete numerical examples are used to evaluate this regularization. We also compare the solutions to the ones based on existing L^2 and H^1 regularization methods.

The fifth section is dedicated to another practical example of inverse problems, namely the fluorescence-enhanced optical tomography problem. A model using the H^s seminorm regularization with computational reconstruction approaches and numerical examples is provided. The last section gives for the conclusions of this work.

To sum up the concepts in this section, the definition of inverse problems and concept of regularization were introduced. After that, different regularization methods in terms of a model problem – deflection of a membrane – were identified. Since all the existing regularization methods have their limitations, a new regularization method should be defined to address those limitations and will be the focus in the next few sections – the H^s seminorm regularization.

2. H^S SEMINORM REGULARIZATION – THEORETICAL ANALYSIS

A new regularization method called H^s seminorm Tikhonov regularization is introduced in this section. As mentioned before, Tikhonov regularization includes *a priori* information to the original optimization problem by adding a regularization term. The regularization functionals listed in the previous section have limitations. Bypassing all the impediments may not be possible but the H^s seminorm as the regularization functional alleviates them to the extent possible. In this section the basic concepts regarding H^s seminorm are introduced, then applied to the nondestructive model problem in the previous section to prove existence and stability for inverse problems.

2.1 Concepts and useful theorems

A Sobolev space is a vector space of functions whose derivatives satisfy some conditions (see Definition 2.12). The H^s space for consideration in the new regularization method is a special Sobolev space and a Hilbert space along with some conditions on fractional derivatives. In this subsection, important concepts about the H^s spaces and seminorms, as well as a few useful theorems, are introduced that will be helpful in proving the existence and stability for inverse problems with H^s seminorm regularization.

2.1.1 Preliminaries

This subsection outlines a few concepts that will be needed in the rest of Subsection 2.1, including the notations of generalized derivatives, the definitions of weak topologies and convergence, compact sets, operators, spaces for Hölder continuous functions, L^p and L^1_{loc} spaces, weak derivatives and classes of domains with different boundaries.

A few notations of generalized derivatives are introduced here [19]:

(i) Let $x = (x_1, x_2, \cdots x_d) \in \mathbb{R}^d$ and u be a function $\mathbb{R}^d \to \mathbb{R}$. The partial derivative of u with respect to x_j, $\forall j$ is denoted by $D_j u = \frac{\partial u}{\partial x_j}$.

(ii) Let $\mathcal{A}_k = \Big\{ \alpha = (\alpha_1, \alpha_2, ..., \alpha_d) : \alpha_j \text{ a nonnegative integer and } |\alpha| := \sum_{j=1}^{d} \alpha_j = k \Big\}$. Let $\alpha \in \mathcal{A}_k$, then the partial derivative of order k of u with respect to x is denoted by:

$$D^\alpha u = D_1^{\alpha_1} D_2^{\alpha_2} \cdots D_d^{\alpha_d} u = \frac{\partial^{|\alpha|} u}{\partial x_1^{\alpha_1} \partial x_2^{\alpha_2} \cdots \partial x_d^{\alpha_d}}.$$

The next few definitions and theorems are important when proving the existence and stability of inverse problems. First are the definitions of weak topology and weak convergence.

Definition 2.1 (Weak topology, [2, 20])**.** The weak topology on a topological or metric space X is the weakest topology with the fewest open sets on X so that each x' in the dual space X' of X is still continuous. The weak topology is weaker than the original topology except for finite dimensional spaces X, where they are equivalent.

Definition 2.2 (Weak convergence, [2])**.** A sequence $\{x_n\}$ on X is said to be weakly convergent to x and denoted by $x_n \rightharpoonup x$ if for every $\phi \in X'$, there is $\phi(x_n) \to \phi(x)$ as $n \to \infty$.

Remark. A sequence $\{x_n\}$ in an inner product space X is said to be weakly convergent to x if for every $y \in X$, we have $(x_n, y) \to (x, y)$ as $n \to \infty$. Here, $(\cdot, \cdot)$ demonstrates the inner product in X.

Theorem 2.1 (Strong and weak convergences, [60])**.** *Strong convergence implies weak convergence, but not vice versa. If* $x_n \rightharpoonup x$, *then* $\{x_n\}$ *is bounded and* $\|x\| \leq \liminf_{n\to\infty} \|x_n\|$.

This theorem defines the relationship between strong convergence (the most common type) and weak convergence. The first part says that we can infer weak convergence from strong convergence, but not vice versa, while the second part proves a strongly bounded property of a weakly convergent sequence.

Next, let us provide the definitions of compact sets. We offer the basic definitions of compact sets, precompact sets and weakly sequentially compact sets.

Definition 2.3 (Compact sets, [2]). Let A be a subset of a metric space X;

(i) A is compact in X if every sequence in A has a convergent subsequence to a point in A,

(ii) A is precompact in X if its closure $\overline{A}$ is compact in X, and

(iii) A is weakly sequentially compact if every sequence in A has a weakly convergent subsequence to a point in A.

In other words, A is precompact if and only if every sequence in $\overline{A}$ has a convergent subsequence to a point in $\overline{A}$.

A space X is reflexive if it has itself as the dual space. For example, all Hilbert spaces are reflexive. The next theorem offers another way to check reflexivity using the definition of sequentially weakly compact sets and spaces.

Theorem 2.2 (Eberlein-Shmulyan, [60]). *A Banach Space X is reflexive if and only if it is locally weakly sequentially compact; in other words, X is reflexive if and only if every strongly bounded sequence in X has a weakly convergent subsequence to a point in X.*

The relationship among spaces includes the use of operators. An operator maps between spaces (sets). Continuous, compact and bounded operators are defined here.

Definition 2.4 (Operators, [2])**.** Let X, Y be normed spaces and f an operator between X and Y:

(i) f is continuous if and only if $x_n \to x$ in X implies that $f(x_n) \to f(x)$ in Y,

(ii) f is compact if, for every A that is bounded in X, $f(A)$ is precompact in Y, and

(iii) f is bounded if, for every A that is bounded in X, $f(A)$ is bounded in Y.

Definition 2.5 (Weakly closed operators, [13, 22])**.** An operator $F : X \to Y$ is weakly closed, if for every weakly convergent sequence $\{x_n\}$ within the domain of F (denoted by $D(F) \subset X$), $x_n \rightharpoonup x$ in X and $F(x_n) \rightharpoonup y$ in Y imply $x \in D(F)$ and $F(x) = y$.

Definition 2.6 (Spaces for Hölder continuous functions, [19])**.** Let Ω be an open subset of $\mathbb{R}^d$, $0 < \alpha \leq 1$, $k \geq 0$ an integer and u a function between Ω and $\mathbb{R}$, then define

$$|u|_{C^{0,\alpha}(\Omega)} := \sup_{x,y\in\Omega,\, x\neq y} \left\{ \frac{|u(x) - u(y)|}{|x - y|^\alpha} \right\}. \tag{2.1}$$

The spaces for Hölder continuous functions are defined as follows:

(i) a function $u \in C(\Omega)$ is in $C^{0,\alpha}(\Omega)$ if $|u|_{C^{0,\alpha}(K)} < \infty$ for every compact subset $K \subset \Omega$,

(ii) a function $u \in C(\overline{\Omega})$ is in $C^{0,\alpha}(\overline{\Omega})$ if $|u|_{C^{0,\alpha}(\overline{\Omega})} < \infty$,

(iii) a function $u \in C^k(\Omega)$ is in $C^{k,\alpha}(\Omega)$ if $|D^a u|_{C^{0,\alpha}(K)} < \infty$ for every compact subset $K \subset \Omega$ and every $a \in \mathcal{A}_k$, and

(iv) a function $u \in C^k(\overline{\Omega})$ is in $C^{k,\alpha}(\overline{\Omega})$ if $|D^a u|_{C^{0,\alpha}(\overline{\Omega})} < \infty$ for every $a \in \mathcal{A}_k$.

Definition 2.7 (L^p spaces, [19]). Let Ω be an open subset of $\mathbb{R}^d$ and $p \geq 1$.

$$\|u\|_{L^p(\Omega)} = \begin{cases} \left(\int_\Omega |u|^p\right)^{\frac{1}{p}}, & \text{if } 1 \leq p < \infty, \\ \inf_{x\in\Omega} \{M : |u(x)| \leq M \ a.e.\}, & \text{if } p = \infty. \end{cases} \tag{2.2}$$

A function $u : \Omega \to \mathbb{R}$ is in $L^p(\Omega)$ if $\|u\|_{L^p(\Omega)} < \infty$.

Definition 2.8 (L^p_{loc} spaces, [19]). Let $\Omega \subset \mathbb{R}^d$ be an open set and $p \geq 1$, a function $u : \Omega \to \mathbb{R}$ is in $L^p_{loc}(\Omega)$ if $u \in L^p(\Omega')$ for every precompact set $\Omega' \subset \Omega$.

Definition 2.9 (Weak derivatives, [2]). A function $v \in L^1_{loc}(\Omega)$ is called the weak derivative of order $|a|$ of $u \in L^1_{loc}(\Omega)$ if

$$\int_\Omega v(x)\phi(x)\,dx = (-1)^{|a|} \int_\Omega u(x) D^a\phi(x)\,dx, \tag{2.3}$$

for all $\phi \in C_0^{|a|}(\Omega)$.

Remark. The weak derivative v of u is also denoted by $D^a u$.

Before concentrating on Sobolev spaces, it is helpful to define several classes of domains based on the regularity conditions of their boundaries. For simplicity, we assume the domain is open and bounded.

Definition 2.10 (Domains with different boundaries, [19]). Let $\Omega \subset \mathbb{R}^d$ be open and bounded,

(i) Ω is of class C^k (i.e. with C^k boundary) if for every $x \in \partial\Omega$, there exists a ball $B = B_r(x)$ and a bijection $H : Q \to B$ such that $H \in C^k(\overline{Q})$, $H^{-1} \in C^k(\overline{B})$, $H(Q_+) = B \cap \Omega$, $H(Q_0) = B \cap \partial\Omega$, where $Q = \{x \in \mathbb{R}^d : |x_j| < 1, \ \forall j\}$, $Q_+ = \{x \in Q : x_d > 0\}$ and $Q_0 = \{x \in Q : x_d = 0\}$,

(ii) Ω is of class $C^{k,\alpha}$ if H and H^{-1} are in $C^{k,\alpha}$, $0 < \alpha \leq 1$, and

(iii) Ω is a Lipschitz domain, if H and H^{-1} are in $C^{0,1}$.

Remark. A unit ball is of class C^{∞}, while every convex domain is a Lipschitz domain.

2.1.2 Sobolev spaces

After introducing the concept of weak derivatives in Definition 2.9, Sobolev spaces can now be described, starting with the definitions of Sobolev norms and spaces, which are the most fundamental concepts.

Definition 2.11 (Sobolev norms, [2])**.** For m a positive integer and $p \geq 1$,

$$\|u\|_{m,p} = \begin{cases} \left(\sum_{0\leq|a|\leq m} \|D^a u\|_p^p\right)^{\frac{1}{p}}, & \text{if } 1 \leq p < \infty, \\ \max_{0\leq|a|\leq m} \|D^a u\|_\infty, & \text{if } p = \infty. \end{cases} \tag{2.4}$$

After formalizing the Sobolev norm, the definition of Sobolev spaces can now be explored.

Definition 2.12 (Sobolev spaces, [2])**.** For m a positive integer and $1 \leq p < \infty$, let

1. $H^{m,p}(\Omega) :=$ the completion of $\{u \in C^m(\Omega) : \|u\|_{m,p} < \infty\}$ with respect to $\|.\|_{m,p}$, and

2. $W^{m,p}(\Omega) := \{u \in L^p(\Omega) : D^a u \in L^p(\Omega) \text{ for } 0 \leq |a| \leq m\}$, where $D^a u$ is the weak partial derivative of order $|a|$.

The first part of the definition for Sobolev spaces utilizes the definition of Sobolev norms, which are the spaces where the Sobolev norms are well-defined. The second part utilizes the weak derivatives directly, which allow an order of up to m. The next theorem gives the equivalence of two definitions of Sobolev spaces. In other words, two definitions still come out with an equivalent space, hence it does not matter in what manner a Sobolev space is defined.

Theorem 2.3 (Meyers and Serrin, [46]). *If* $1 \leq p < \infty$, *then*

$$H^{m,p}(\Omega) = W^{m,p}(\Omega). \tag{2.5}$$

The most significant concepts in this subsection, fractional Sobolev spaces and norms, are examined here. These are the ones that we actually use as the H^s seminorm regularization functional.

Definition 2.13 (Fractional Sobolev spaces, [47]). Let Ω be a domain in $\mathbb{R}^d$ and $s \in (0,1)$, for any $p \in [1, \infty)$, $W^{s,p}(\Omega)$ is defined as follows:

$$W^{s,p}(\Omega) = \left\{ u \in L^p(\Omega) : \frac{|u(x) - u(y)|}{|x-y|^{\frac{d}{p}+s}} \in L^p(\Omega \times \Omega) \right\}. \tag{2.6}$$

$W^{s,p}(\Omega)$ is an intermediary Banach space between $L^p(\Omega)$ and $W^{1,p}(\Omega)$.

Definition 2.14 (Fractional Sobolev norms, [47]). Let Ω be a domain in $\mathbb{R}^d$ and $s \in (0,1)$, for any $p \in [1, \infty)$,

$$\|u\|_{W^{s,p}(\Omega)} := \left(\int_\Omega |u|^p \, dx + \int_\Omega \int_\Omega \frac{|u(x) - u(y)|^p}{|x-y|^{d+sp}} \, dxdy \right)^{\frac{1}{p}} \tag{2.7}$$

where

$$|u|_{W^{s,p}(\Omega)} := \left(\int_\Omega \int_\Omega \frac{|u(x) - u(y)|^p}{|x-y|^{d+sp}} \, dxdy \right)^{\frac{1}{p}} \tag{2.8}$$

is also called Gagliardo seminorm of u.

Although general fractional Sobolev spaces are worth study, the focus here is on a special space for $p = 2$. When $p = 2$, the fractional Sobolev space becomes a

Hilbert space H^s. In other words, H^s is a complete inner product space with respect to the induced distance by the inner product, which is also reflexive. Because of these properties, H^s space is the selected one in which H^s seminorm regularization is utilized.

Definition 2.15 (H^s spaces and norms)**.** Let Ω be a domain in $\mathbb{R}^d$ and $s \in (0,1)$, $H^s(\Omega) = W^{s,2}(\Omega)$, which is an intermediary Banach space between $L^2(\Omega)$ and $H^1(\Omega) = W^{1,2}(\Omega)$. The norm:

$$\|u\|_{H^s(\Omega)} := \left(\int_\Omega |u|^2 \; dx + \int_\Omega \int_\Omega \frac{|u(x) - u(y)|^2}{|x-y|^{d+2s}} \;\; dxdy \right)^{\frac{1}{2}} \tag{2.9}$$

is equipped in $H^s(\Omega)$, and the seminorm is defined as follows:

$$|u|_{H^s(\Omega)} := \left(\int_\Omega \int_\Omega \frac{|u(x) - u(y)|^2}{|x-y|^{d+2s}} \;\; dxdy \right)^{\frac{1}{2}}. \tag{2.10}$$

2.1.3 Sobolev embedding theorems

Embedding involves a subspace being mapped to itself in a larger space by a continuous identity operator. In addition, if the identity operator is compact, the embedding is compact, too. Through embedding, a subspace with special properties can preserve general properties of the entire space.

Definition 2.16 (Embeddings, [2])**.** A normed space X is embedded in a normed space Y, denoted by $X \to Y$ if:

1. X is a subspace of Y, and

2. the identity operator I is continuous, where I is defined between X and Y by $Iu = u$ for $\forall u \in X$.

X is compactly embedded in Y if the embedding operator I is compact.

Remark. The second part of the definition is equivalent to the statement that there exists a constant C such that $\|Iu\|_Y \leq C\|u\|_X$, for $\forall u \in X$.

Theorem 2.4 (Sobolev embedding theorems, [2]). *Let Ω be an open and bounded Lipschitz domain in $\mathbb{R}^d$, $m \geq 1$ an integer and $1 \leq p \leq \infty$.*

(i) *If either $mp > d$ or $m = d$ and $p = 1$, then*

$$W^{m,p}(\Omega) \to L^q(\Omega) \qquad \text{for } \; p \leq q \leq \infty \tag{2.11}$$

(ii) *If $mp = d$ then*

$$W^{m,p}(\Omega) \to L^q(\Omega) \qquad \text{for } \; p \leq q < \infty \text{ compactly} \tag{2.12}$$

(iii) *If $mp < d$ then*

$$W^{m,p}(\Omega) \to L^q(\Omega) \qquad \text{for } \; p \leq q < p^\star = \frac{np}{d - mp} \text{ compactly} \tag{2.13}$$

The Sobolev embedding theorems for integer-order Sobolev spaces are the building blocks used to construct embedding theorems for fractional-order Sobolev spaces. Before stating the embedding theorems, the following definition is offered as a constraint for domains: an extension domain for some space is simply a domain so that each function defined on the domain in that space is extensible to $\mathbb{R}^d$.

Definition 2.17 (Extension domain, [47, 55]). Let $s \in (0, 1)$ and $p \in [1, \infty)$, a domain $\Omega \subset \mathbb{R}^d$ is an extension domain for $W^{s,p}$, if there exists a constant $C > 0$

such that for each function $u \in W^{s,p}(\Omega)$, there exists $\bar{u}$ such that $\bar{u}|_\Omega = u$, and there exists a constant $C > 0$ such that

$$\|\bar{u}\|_{W^{s,p}(\mathbb{R}^d)} \leq C\|u\|_{W^{s,p}(\Omega)}. \tag{2.14}$$

Remark. Every Lipschitz domain is an extension domain. Please refer to [40, 47] for detailed discussions.

Several embedding theorems for fractional Sobolev spaces are presented in the next few theorems. Similar to integer-valued Sobolev embedding theorems, there are Sobolev embedding theorems that are applicable in different situations based on whether sp is less than, equal to or greater than d, where s, p and d are defined in Definition 2.13.

Theorem 2.5 (Sobolev embedding $W^{s,p}(\Omega) \to W^{s,p}(\mathbb{R}^d)$, [47])**.** *Let $s \in (0,1)$, $p \in [1,\infty)$ and $\Omega \subseteq \mathbb{R}^d$ be a Lipschitz domain. Then $W^{s,p}(\Omega)$ is continuously embedded in $W^{s,p}(\mathbb{R}^d)$, namely for each $u \in W^{s,p}(\Omega)$, there exists $\bar{u}$ such that $\bar{u}|_\Omega = u$, and there exists a constant $C > 0$ such that*

$$\|\bar{u}\|_{W^{s,p}(\mathbb{R}^d)} \leq C\|u\|_{W^{s,p}(\Omega)}. \tag{2.15}$$

Theorem 2.6 (Sobolev embedding for $sp < d$, [47])**.** *Let $0 < s < 1$, $p \geq 1$ such that $sp < d$ and $\Omega \subseteq \mathbb{R}^d$ be a bounded extension domain for $W^{s,p}$. Then $W^{s,p}(\Omega)$ is continuously embedded in $L^q(\Omega)$, where $q \in [1, p^\star := \frac{dp}{d-sp}]$, namely for each $u \in W^{s,p}(\Omega)$, there exists $\bar{u}$ such that $\bar{u}|_\Omega = u$, and there exists a constant $C > 0$ such that*

$$\|\bar{u}\|_{L^q(\Omega)} \leq C\|u\|_{W^{s,p}(\Omega)}. \tag{2.16}$$

Theorem 2.7 (Sobolev embedding for $sp = d$, [47])**.** *Let $0 < s < 1$, $p \geq 1$ such* *that $sp = d$ and $\Omega \subseteq \mathbb{R}^d$ be a bounded extension domain for $W^{s,p}$. Then $W^{s,p}(\Omega)$ is continuously embedded in $L^q(\Omega)$ for every $q \in [1, \infty)$, namely for each $u \in W^{s,p}(\Omega)$, there exists $\bar{u}$ such that $\bar{u}|_\Omega = u$, and there exists a constant $C > 0$ such that*

$$\|\bar{u}\|_{L^q(\Omega)} \leq C\|u\|_{W^{s,p}(\Omega)}. \tag{2.17}$$

Theorem 2.8 (Sobolev embedding for $sp > d$, [47]). *Let $0 < s < 1$, $p \geq 1$ such that $sp > d$ and $\Omega \subseteq \mathbb{R}^d$ a Lipschitz domain for $W^{s,p}$. Then $W^{s,p}(\Omega)$ is continuously embedded in $C^{0,\alpha}(\Omega) \subset C^0(\Omega)$, where $\alpha := \frac{sp-d}{p}$. In other words, for each $u \in W^{s,p}(\Omega)$, there exists $\bar{u}$ such that $\bar{u}|_\Omega = u$, and there exists a constant $C > 0$ such that*

$$\|\bar{u}\|_{C^{0,\alpha}(\Omega)} \leq C\|u\|_{W^{s,p}(\Omega)}. \tag{2.18}$$

Here $\|\bar{u}\|_{C^{0,\alpha}(\Omega)} = \|\bar{u}\|_{L^\infty(\Omega)} + |\bar{u}|_{C^{0,\alpha}(\Omega)}$. In addition, $W^{s,p}(\Omega)$ is continuously embedded in $L^q(\Omega)$ for every $q \geq 1$. For each $u \in W^{s,p}(\Omega)$, there exists $C_2 > 0$ so that

$$\|u\|_{L^q(\Omega)} \leq C_2\|u\|_{W^{s,p}(\Omega)}. \tag{2.19}$$

The next few theorems state compact embedding results for fractional Sobolev spaces.

Theorem 2.9 (Compact embedding, [47]). *Let $0 < s < 1$, $p \geq 1$, $1 \leq q \leq p$ and $\Omega \subseteq \mathbb{R}^d$ be a bounded extension domain for $W^{s,p}$ and $\mathcal{I} \subset L^p(\Omega)$ be bounded. Then $\mathcal{I}$ is precompact in $L^q(\Omega)$ if $\sup_{u \in \mathcal{I}} |u|_{W^{s,p}(\Omega)} < \infty$.*

Remark. Equivalently, Theorem 2.9 demonstrates that $W^{s,p}(\Omega)$ is compactly embedded in $L^q(\Omega)$ for $q \in [1, p]$.

Proof. For each $u \in W^{s,p}(\Omega)$, the identity operator $I : W^{s,p}(\Omega) \to L^q(\Omega)$ for $q \in [1, p]$

is defined as $Iu = u$. $W^{s,p}(\Omega)$ is compactly embedded in $L^q(\Omega)$ for $q \in [1, p]$ if and only if I is compact. Based on Definition 2.4, I is compact if and only if $I(\mathcal{I}) = \mathcal{I}$ is precompact in $L^q(\Omega)$ for each bounded $\mathcal{I} \subset W^{s,p}(\Omega)$. Since Theorem 2.9 states that $\mathcal{T}$ is precompact in $L^q(\Omega)$ for each bounded $\mathcal{T} \subset W^{s,p}(\Omega)$, $W^{s,p}(\Omega)$ is compactly embedded in $L^q(\Omega)$ for $q \in [1, p]$. □

Theorem 2.10 (Compact embedding for $sp < d$, [47])**.** *Let $0 < s < 1$, $p \geq 1$ such that $sp < d$, $1 \leq q \leq p^\star = \frac{dp}{d-sp}$ and $\Omega \subseteq \mathbb{R}^d$ be a bounded extension domain for $W^{s,p}$ and $\mathcal{I} \subset L^p(\Omega)$ be bounded. Then $\mathcal{I}$ is pre-compact in $L^q(\Omega)$ if $\sup_{u \in \mathcal{I}} |u|_{W^{s,p}(\Omega)} < \infty$.*

Remark. Equivalently, Theorem 2.10 demonstrates that $W^{s,p}(\Omega)$ is compactly embedded in $L^q(\Omega)$ for $sp < d$ and $q \in [1, p^\star]$.

The fractional embedding theorems are substantial in the theory of fractional Sobolev spaces and a fundamental basis for the existence and stability of the model inverse problems, as well.

2.1.4 Other useful theorems

The next few definitions and theorems are related to Meyers' theorem, which is vital in proving the existence and stability of inverse problems. First, some definitions used in Meyers' theorem are provided. Consider linear differential operators L of the form:

$$Lu = \nabla \cdot A \nabla u,$$

where matrix A and function u are complex valued.

Definition 2.18 (Alternative uniform ellipticity conditions)**.** A complex matrix A is said to satisfy uniform elliptic conditions if there exist H, R so that

$$A = H + R,$$

where H is Hermitian and H, R satisfy the following inequalities for some $0 < \theta \leq 1$ and $\Lambda \geq \lambda > 0$:

$$\lambda \|\xi\|_{L^2}^2 \leq (H\xi, \xi) \leq \Lambda \|\xi\|_{L^2}^2$$
$$\|R\| \leq (1-\theta)\lambda,$$

where $\|R\| = \max_{\|\xi\|=1} \|R\xi\|_{L^2}$ for all $\xi \in \mathbb{R}^d$.

Definition 2.19. Let $q \in (1, \infty)$ and $n \in \mathbb{N}$, $n > 0$, then q' and q^* are defined as follow:

(i) $q' = \frac{q}{q-1}$, which indicates $\frac{1}{q} + \frac{1}{q'} = 1$,

(ii)
$$q^* = \begin{cases} \frac{nq}{n-q}, & \text{if } q < n, \\ \text{any number}, & \text{if } q \geq n. \end{cases}$$

The main part of Meyers' theorem is presented next. Essentially, it indicates that the connection between a solution of a partial differential equation and the coefficient and right-hand sides of that equation provided a list of conditions. If the coefficient A in the definition of the operator L satisfies the conditions in Definition 2.18, and if the right-hand sides satisfy some conditions as well (as described in the theorem), then the gradient of the solution is bounded by the right-hand sides.

Theorem 2.11 (Meyers' theorem, [45])**.** *Let Ω be a bounded domain of class C^q for some $q \in (2, \infty)$. Consider the differential equation*

$$Lu = \nabla \cdot A \nabla u = \nabla \cdot \vec{f} + h, \tag{2.20}$$

where the complex matrix A satisfies Condition 2.18 a.e. for $\Lambda = 1$. Then there *exists a unique solution in* $W_0^{1,p}$ *for* (2.20) *for every* $\vec{f} \in L^p$ *and every* $h \in L^r$ *where* $r^* \geq p$*, provided*

$$q' \leq Q' < p < Q \leq q,$$

where $Q > 2$ *only depends on the domain* Ω *and* $\theta\lambda$*, such that* $Q \to q$ *as* $\theta\lambda \to 1$ *and* $Q \to 2$ *as* $\theta\lambda \to 0$*. The following condition holds for the solution:*

$$\|\nabla u\|_{L^p} \leq C\{\|\vec{f}\|_{L^p} + \|h\|_{L^r}\}$$

for some constant C *that depends only on the domain,* $\theta\lambda$*,* p *and* r*.*

Here we would also like to state Meyers' theorem that is formulated in [35, 52].

Theorem 2.12 (Meyers' theorem)**.** *Let* Ω *be a bounded Lipschitz domain in* $\mathbb{R}^d$*. Consider the differential equation:*

$$\nabla \cdot \sigma \nabla u = \nabla \vec{f} + h, \tag{2.21}$$

where $\sigma \in L^\infty(\Omega)$ *satisfies* $\lambda < \sigma < \frac{1}{\lambda}$ *for some constant* $\lambda \in (0, 1)$*. For fixed* λ*, there exists a constant* $Q > 2$ *that only depends on* λ *and* d*, such that for any* $2 < r < Q$*,* $Q \to 2$ *as* $\lambda \to 0$ *and* $Q \to \infty$ *as* $\lambda \to 1$*, then for any* $2 < q < Q$*, there exists a solution* u *in* $W_0^{1,r}$ *for* (2.21) *for every* $\vec{f} \in (L^r(\Omega))^d$ *and every* $h \in L^r(\Omega)$*. The solution satisfies:*

$$\|u\|_{W^{1,r}} \leq C\{\|\vec{f}\|_{L^r(\Omega)} + \|h\|_{L^r(\Omega)}\}$$

for some constant C *that depends only on the domain,* λ*,* d*,* q *and* σ*.*

The last thing to demonstrate in this subsection is the Poincaré inequality.

Theorem 2.13 (Poincaré inequality, [19])**.** *If* Ω *is bounded, and* $p \geq 1$*, then there* *exists a constant c such that*

$$\|u\|_{L^p} \leq c\|\nabla u\|_{L^p}, \forall u \in W_0^{1,p}(\Omega). \tag{2.22}$$

2.2 The existence and stability for the model problem

After introducing the definitions and theorems about fractional Sobolev spaces, and in particular H^s spaces, the tools to demonstrate the existence of solutions to the model problem are now available.

2.2.1 General form of the model problem

First, recall the general form of an inverse problem:

$$F(q) = z, \tag{2.23}$$

where $F : X \to Y$ is a nonlinear operator for Hilbert spaces X and Y. Assuming that an F that maps the parameter sought to the measurements already gathered can be defined, then (2.23) sketches an inverse problem in a very general way. This is also very difficult to solve exactly.

Tikhonov regularization using least square method makes (2.23) well-posed. Thus, the following minimization problem is an approximation of the original nonlinear equation (2.23):

$$\min_{u,q} m(q, z^\delta) + \beta r(q), \tag{2.24}$$

where $\beta > 0$ is a small number, called the regularization parameter. $m(q, z^\delta)$ measures the distance between $F(q)$ and z, which depends on the solution u of the forward problem which itself depends on q. A common choice for these functionals is to use the natural norms, in which case (2.24) can be written as:

$$\min_{u,q} \frac{1}{2}\|F(q) - z\|_Y^2 + \frac{\beta}{2}\|q\|_X^2. \tag{2.25}$$

Now turn to the model problem of determining the elastic properties of a membrane by casting certain forces and measuring the corresponding deflections. In this case, q is the elastic property of a membrane, or its stiffness. z is the corresponding measurement of deflections. F is the map between $q \in X$ and $z \in Y$.

A mathematical formulation is as follow: for the considered membrane, the deflection $u(x)$ is subject to a Poisson equation with Dirichlet boundary condition:

$$-\nabla \cdot q(x)\nabla u(x) = f(x), \quad x \in \Omega \tag{2.26}$$

$$u(x) = 0, \quad x \in \partial\Omega \tag{2.27}$$

where $x \in \Omega$, and $f(x)$ is the given force, and $q(x)$ is the stiffness of the membrane we seek.

Let $\mathcal{K} = \{q \in L^\infty(\Omega) : c_0 \leq q \leq c_1 \ a.e.\}$ be the admissible set for the parameter q. Here this set is closed and convex.

The weak formulation is reached by taking the L^2 inner product on both sides of (2.26) with a test function $v(x) \in H_0^1(\Omega)$:

$$\int q\nabla u \cdot \nabla v = \int fv dx \qquad \forall v \in H_0^1(\Omega). \tag{2.28}$$

The optimization problem is:

$$\min_{q} \frac{1}{2}\|F(q) - z\|_Y^2 + \frac{\beta}{2}\|q\|_X^2 \qquad \text{over the domain of } F \tag{2.29}$$

for some Hilbert spaces X and Y. Typically, Y can be $L^2(\Omega)$ or $H^1(\Omega)$. In this case, X is set to be $X = W^{s,2}(\Omega) =: H^s(\Omega)$, for some $0 < s < 1$.

We define the domain of F as $D(F) := X \cap \mathcal{K}$. Notice that the admissible set $\mathcal{K}$ and $D(F)$ are closed. Let $\mathcal{S}$ be an open set satisfying $\mathcal{K} \subset \mathcal{S}$, where the operator F is well defined. For the remainder of this work, we will specifically choose $\mathcal{S} = \{q \in L^\infty(\Omega) : c_0/2 < q < 2c_1 \ a.e.\}$. After that, we may deal with the open extended domain of F, namely $U := X \cap \mathcal{S}$ (see [18] for example).

Lemma 2.14. *Let $0 < s < 1$, Ω be a bounded Lipschitz domain and d be the dimension of Ω, then the extended domain $U = H^s(\Omega) \cap \{q \in L^\infty(\Omega) : c_0/2 < q < 2c_1 \ a.e.\}$ is open under H^s norms when $s > \frac{d}{2}$.*

Proof. Based on Theorem 2.8, $H^s(\Omega)$ is continuously embedded in $L^\infty(\Omega)$ when $s > \frac{d}{2}$. Equivalently, for each $x \in H^s(\Omega)$, there exists $C_2 > 0$ so that

$$\|x\|_{L^\infty(\Omega)} \leq C_2 \|x\|_{H^s(\Omega)}. \tag{2.30}$$

Therefore for any $q \in U$, and any q' in the ball $B_\epsilon(q) := \{q' : \|q' - q\|_{H^s(\Omega)} \leq \epsilon\}$, $\|q' - q\|_{L^\infty(\Omega)} \leq C_2 \|q' - q\|_{H^s(\Omega)} \leq C_2 \epsilon$. In that case, we may choose an ϵ small enough so that $B_\epsilon(q) \subset U$, which proves that U is open under H^s norms when $s > \frac{d}{2}$. $\square$

Remark. U is not open under H^s norms when $d > 1$. Since when $d = 2$, for example, Lemma 2.14 requires that $s > \frac{d}{2} = 1$, which contradicts to $0 < s < 1$.

For the model problem (2.26), the operator F may more specifically be defined as:

$$F(q) := u(x), \tag{2.31}$$

where $u(x)$ solves (2.28) for given fixed F and the argument q of F.

2.2.2 Some properties for the operator F

To prove the existence of a solution for the model problem, some properties of the operator (2.31) for different spaces X and Y are evaluated in this subsection, including weak closedness, continuity and differentiability. The techniques used in this subsection closely follow [35, 52].

2.2.2.1 Weak closedness

The following lemma claims that the operator (2.31) is weakly closed on $D(F)$ if $X = H^s(\Omega)$ for $0 < s < 1$ and $Y = H^1(\Omega)$ or $L^2(\Omega)$.

Lemma 2.15. *Let Ω be a bounded Lipschitz domain:*

$$X = H^s(\Omega) \quad \textit{for } s \in (0,1),$$

$$Y = H^1(\Omega) \quad \textit{or} \quad L^2(\Omega).$$

Then $F : D(F) \subset X \to Y$ defined in (2.31) *is weakly closed.*

Proof. Let $\{q_n\} \subset D(F)$ in X be a weakly convergent sequence; $q_n \rightharpoonup \bar{q}$ and $u_n := F(q_n)$. Based on Definition 2.5 of weakly closed operators, there are two major claims. First claim: $\bar{q} \in D(F)$.

Since $\{q_n\}$ is a weakly convergent sequence, based on Theorem 2.1, $\{q_n\}$ is strongly bounded. Then, since X is a Hilbert space (hence reflexive), based on Theorem 2.2, $\{q_n\}$ contains a subsequence which converges weakly to an element of X, namely $\bar{q}$. Additionally, since $\{q_n\}$ is weakly convergent, $q_n \rightharpoonup \bar{q}$, and $\bar{q} \in X$.

Notice also that the strong boundedness of $\{q_n\}$ in X implies that the L^2 norms and Gagliardo seminorms of $\{q_n\}$ are bounded in $L^2(\Omega)$ and $L^2(\Omega \times \Omega)$, respectively. Then, q_n is in a bounded subset A of $L^2(\Omega)$. Based on Theorem 2.9, $X = H^s(\Omega)$ is compactly embedded in $L^2(\Omega)$, which implies if $q_n \rightharpoonup \bar{q}$ in X, then $q_n \to \bar{q}$ in $L^2(\Omega)$.

If $\bar{q} \notin D(F)$, then there exists a subset M of $\mathbb{R}^d$ with nonzero measure, such that $\bar{q}(x) > c_1, \quad \forall x \in M$. Defining $\chi_M \in L^2$ to be the characteristic function over M, then $\int_\Omega (q_n - \bar{q})\chi_M \nrightarrow 0$, for n large enough, which contradicts to the convergence of $\{q_n\}$ in $L^2(\Omega)$. A similar argument holds for $\bar{q}(x) < c_0$ for some x. Hence, $\bar{q} \in D(F)$.

Second claim: $u_n \rightharpoonup \bar{u}$, and $F(\bar{q}) = \bar{u}$. The initial step is to prove that there exists a subsequence $\{u_{n_k}\}$ of $\{u_n\}$, such that $u_{n_k} \rightharpoonup \bar{u}$ in Y, and $F(\bar{q}) = \bar{u}$.

In (2.28), let $v = u$, then

$$\begin{aligned} \int_\Omega q|\nabla u|^2 &\leq \|f\|_{L^2(\Omega)}\|u\|_{L^2(\Omega)} \quad \text{by Cauchy-Schwarz inequality} \\ &\leq \|f\|_{L^2(\Omega)}\|u\|_{H^1(\Omega)}. \end{aligned}$$

Since $c_0 \leq q \leq c_1$,

$$c_0 \int_\Omega |\nabla u|^2 \leq \int_\Omega q|\nabla u|^2.$$

Based on Poincaré Inequality (Theorem 2.13) and $u = 0$ on $\partial\Omega$,

$$c_2\|u\|_{H^1(\Omega)} \leq \|\nabla u\|_{L^2(\Omega)} \leq c_3\|u\|_{H^1(\Omega)},$$

for some constant c_2 and c_3. Thus:

$$c\|u\|_{H^1}^2 \leq \int_\Omega q|\nabla u|^2 \, dx$$

for some constant c. Together,

$$\begin{aligned} \|u\|_{H^1(\Omega)}^2 &\leq C\|f\|_{L^2(\Omega)}\|u\|_{H^1(\Omega)}, \\ \|u\|_{H^1(\Omega)} &\leq C\|f\|_{L^2(\Omega)} = C'. \end{aligned} \tag{2.32}$$

In other words, u is uniformly bounded in $H^1(\Omega)$, and in particular $\{u_n\}$ is uniformly bounded in $H^1(\Omega)$. Based on Theorem 2.2, Y is a Hilbert space (hence, reflexive), and there exists a subsequence $\{u_{n_k}\}$ of $\{u_n\}$ such that $u_{n_k} \rightharpoonup \bar{u}$ in $H^1(\Omega)$. Based on Theorem 2.4, $u_{n_k} \to \bar{u}$ in $L^2(\Omega)$. Thus,

$$u_{n_k} \rightharpoonup \bar{u} \text{ in } Y(\Omega). \tag{2.33}$$

The next thing to check is $F(\bar{q}) = \bar{u} = u(\bar{q})$.

$$\begin{aligned} &\int_\Omega q_{n_k} \nabla u_{n_k} \cdot \nabla v \, dx - \int_\Omega \bar{q} \nabla \bar{u} \cdot \nabla v \, dx \\ &= \int_\Omega q_{n_k} \nabla (u_{n_k} - \bar{u}) \cdot \nabla v \, dx + \int_\Omega (q_{n_k} - \bar{q}) \nabla \bar{u} \cdot \nabla v \, dx. \end{aligned} \tag{2.34}$$

Since $u_{n_k} \to \bar{u} \quad$ in $L^2(\Omega)$, and $u_{n_k} \rightharpoonup \bar{u} \quad$ in $H^1(\Omega)$, based on the definition of weak convergence, $\nabla u_{n_k} \rightharpoonup \nabla \bar{u} \quad$ in $L^2(\Omega)$.

Since $c_0 \leq q \leq c_1 \quad \forall q$, and $\nabla v \in L^2(\Omega)$, then

$$\int_\Omega q_{n_k} \nabla (u_{n_k} - \bar{u}) \cdot \nabla v \, dx = \int_\Omega \nabla (u_{n_k} - \bar{u}) \cdot q_{n_k} \nabla v \, dx \to 0,$$

so

$$\int_\Omega q_{n_k} \nabla (u_{n_k} - \bar{u}) \cdot \nabla v \, dx \to 0. \tag{2.35}$$

The second part of (2.34) is estimated.

First, based on Theorem 2.12, for each q_{n_k} there exists a solution in $W_0^{1,t}(\Omega)$, which by definition is $u_{n_k} = F(q_{n_k})$. Here $2 < t < Q$, for some $Q \in (2, \infty)$. Therefore, since $\{u_{n_k}\}$ is a convergent sequence and $W_0^{1,t}(\Omega)$ is a Banach space, $\bar{u} \in W_0^{1,t}(\Omega)$, namely,

$$u_{n_k} \rightharpoonup \bar{u} \text{ in } W^{1,t} \qquad \text{for some } \; t > 2. \tag{2.36}$$

Thus, based on Theorem 2.1,

$$\|\nabla \bar{u}\|_{L^t} \leq C. \tag{2.37}$$

In addition, based on Theorem 2.9, let $p = 2$,

$$q_{n_k} \rightharpoonup \bar{q} \quad \text{in} \quad H^s(\Omega) \Rightarrow q_{n_k} \to \bar{q} \quad \text{in} \quad L^2(\Omega). \tag{2.38}$$

Let $\frac{1}{r} = \frac{1}{2} - \frac{1}{t}$, then $r > 2$,

$$\int_\Omega \left|q_{n_k} - \bar{q}\right|^r dx = \int_\Omega \left|q_{n_k} - \bar{q}\right|^2 \left|q_{n_k} - \bar{q}\right|^{r-2} dx. \tag{2.39}$$

Since $\forall q, c_0 \leq q \leq c_1, a.e.,$ $\left|q_{n_k} - \bar{q}\right|^{r-2} \leq C$, for some C. So

$$\int_\Omega \left|q_{n_k} - \bar{q}\right|^r dx \leq C \int_\Omega \left|q_{n_k} - \bar{q}\right|^2 dx \to 0. \tag{2.40}$$

Then,

$$\int_\Omega (q_{n_k} - \bar{q}) \nabla \bar{u} \cdot \nabla v \, dx \leq \|q_{n_k} - \bar{q}\|_{L^r} \|\nabla \bar{u}\|_{L^t} \|\nabla v\|_{L^2} \to 0. \tag{2.41}$$

Based on the estimation of (2.35) and (2.41),

$$\int_\Omega q_{n_k} \nabla u_{n_k} \cdot \nabla v \, dx - \int_\Omega \bar{q} \nabla \bar{u} \cdot \nabla v \, dx \to 0. \tag{2.42}$$

By definition, $u_{n_k} = F(q_{n_k})$, $\int_\Omega q_{n_k} \nabla u_{n_k} \cdot \nabla v \, dx = \int_\Omega f v \, dx$,

$$\int_\Omega \bar{q} \nabla \bar{u} \cdot \nabla v \, dx = \int_\Omega f v \, dx.$$

Therefore, $\bar{u} = F(\bar{q})$.

Now, since for each subsequence of $\{u_n = F(q_n)\}$, the same procedure can be followed to identify a subsequence which converges to $\bar{u} = F(\bar{q})$.

If $u_n = F(q_n)$ does not converge weakly to $\bar{u} = F(\bar{q})$, then there exists an ϵ and a function $\phi \in Y$ such that $\forall N \in \mathbb{N}$, there exists an $n_N > N$, and $|(u_{n_N} - \bar{u}, \phi)| > \epsilon$. Thus, $\{u_{n_N},\ N \in \mathbb{N}\}$ is a subsequence of $\{u_n\}$. By following the same procedure as above, a subsequence that converges to $\bar{u} = F(\bar{q})$ can be found, though this is a contradiction. This gives $u_n = F(q_n) \rightharpoonup \bar{u} = F(\bar{q})$.

This completes the proof.

□

Remark. In general, F is not weakly closed on U, the extended domain of F. For example, F is not weakly closed on $U = X \cap \mathcal{S}$ because U is not closed.

The next lemma is almost the same as Lemma 2.15, with the exception that $m \in \mathbb{N}$.

Lemma 2.16. *Let n be the dimension of the domain Ω.*

$$X = H^m(\Omega) \quad \textit{for } m \in \mathbb{N},$$
$$Y = H^1(\Omega) \quad \textit{or} \quad L^2(\Omega).$$

Then $F : D(F) \subset X \to Y$ defined in (2.31) *is weakly closed.*

Proof. Similar proof as Lemma 2.15, using Theorem 2.4. □

Weak closedness is an essential characteristic for an operator. Only when an operator (defined in (2.23)) is weakly closed may the journey of proof to the existence for solutions of inverse problems continue. In this case, weak closedness is a fundamental lemma and will be used in the next few lemmas for continuity and differentiability.

2.2.2.2 *Continuity of the operator*

In this subsection, the continuity of $F(q)$ is considered. We would like to study the continuity of F on $U = X \cap \mathcal{S}$, the extended domain of F, when $X = H^s(\Omega)$. As stated in Lemma 2.14 and the remark below that lemma, U is open only when d, the dimension of Ω, is 1, and $s > d/2$. Accordingly, the results in the remainder of the subsection are only valid for $d = 1$.

Lemma 2.17. *Let* $\Omega \subset \mathbb{R}$*:*

$$X = H^s(\Omega) \quad \textit{for } s \in (1/2, 1),$$
$$Y = H^1(\Omega) \quad \textit{or} \quad L^2(\Omega).$$

Then for $F : U \subset X \to Y$ *(in* (2.31)*) and* Q *in Meyers' Theorem (Theorem 2.12):*

1. *F is continuous in the $L^2(\Omega)$ norm, namely for every convergent sequence $\{q_n\}$ in $U \subset X$, $q_n \to \bar{q}$, $F(q_n) \to F(\bar{q})$ in $L^2(\Omega)$ norm;*

2. *for any $p \in (\frac{2Q}{Q-2}, \infty)$, and $q, q + \delta q \in U \cap L^p(\Omega)$,*

$$\|F(q + \delta q) - F(q)\|_{H^1(\Omega)} \le C\|\delta q\|_{L^p(\Omega)}; \tag{2.43}$$

3. *for any $p \in (\frac{4Q}{Q-2}, \infty)$, and $q, q + \delta q \in U \cap L^p(\Omega)$, there exists $t \in (2, Q)$ such that*

$$\|F(q + \delta q) - F(q)\|_{W^{1,t}(\Omega)} \le C\|\delta q\|_{L^p(\Omega)}. \tag{2.44}$$

Proof. We may use a similar procedure for the first part of Lemma 2.17 as the one that is used in the proof of Lemma 2.15, although the domain of F here is U, the extended domain of F, instead of $D(F)$.

Now for the second part, a similar proof is used as in [35].

$$\int_\Omega q\nabla F(q)\cdot\nabla v\ dx = \int_\Omega fv\ dx \quad \forall v\in H_0^1(\Omega) \tag{2.45}$$
$$\int_\Omega (q+\delta q)\nabla F(q+\delta q)\cdot\nabla v\ dx = \int_\Omega fv\ dx \quad \forall v\in H_0^1(\Omega). \tag{2.46}$$

Therefore,

$$\int_\Omega q\nabla(F(q)-F(q+\delta q))\cdot\nabla v\ dx = \int_\Omega \delta q\nabla F(q+\delta q)\cdot\nabla v\ dx \quad \forall v\in H_0^1(\Omega). \tag{2.47}$$

Let $v = F(q)-F(q+\delta q)\in H_0^1(\Omega)$,

$$\begin{aligned}\int_\Omega q|\nabla(F(q){-}F(q+\delta q))|^2\ dx &= \int_\Omega \delta q\nabla F(q+\delta q)\cdot\nabla(F(q)-F(q+\delta q))\ dx\\ &\le \|\delta q\|_{L^p(\Omega)}\|\nabla F(q+\delta q)\|_{L^r(\Omega)}\|\nabla(F(q)-F(q+\delta q))\|_{L^2(\Omega)}\end{aligned}$$

where $\frac{1}{r}+\frac{1}{p}=\frac{1}{2}$. Since $p>\frac{2Q}{Q-2}$, i.e. $\frac{1}{p}+\frac{1}{Q}<\frac{1}{2}$, $2<r<Q$. Using Theorem 2.12 on (2.46), there exists a constant C such that

$$|\nabla F(q+\delta q)|_{L^r(\Omega)} \le C\|f\|_{L^r(\Omega)} = C'. \tag{2.48}$$

Using (2.48) in the previous inequality and considering the Poincaré inequality (Theorem 2.13),

$$\|F(q)-F(q+\delta q)\|_{H^1(\Omega)} \le C'\|\delta q\|_{L^p(\Omega)}. \tag{2.49}$$

This proves the second part of this lemma.

For the third part, a similar proof is used as in [35]. For any $p\in\left(\frac{4Q}{Q-2},\infty\right)$, let t be the solution of $\frac{1}{t}+\frac{1}{p}=\frac{1}{2}$, then $t\in(2,\frac{4Q}{Q+2})\subset(2,Q)$. Using Theorem 2.12 on

(2.47),

$$\|F(q) - F(q+\delta q)\|_{W^{1,t}(\Omega)} \leq C\|\delta q \nabla F(q+\delta q)\|_{L^t(\Omega)}. \tag{2.50}$$

To estimate the right hand side of (2.50), based on Theorem 2.12 and Hölder's inequality, for any $a > 1$, and $\frac{1}{a} + \frac{1}{b} = 1$, we have,

$$\begin{aligned}
\int |\delta q \nabla F(q+\delta q)|^t \, dx &= \int |\delta q|^t |\nabla F(q+\delta q)|^t dx &(2.51)\\
&\leq \left(\int |\delta q|^{ta} \, dx\right)^{\frac{1}{a}} \left(\int |\nabla F(q+\delta q)|^{tb} \, dx\right)^{\frac{1}{b}} &(2.52)\\
&\leq C \left(\int |\delta q|^{at} \, dx\right)^{\frac{1}{a}}. &(2.53)
\end{aligned}$$

Let $t' = \frac{2t}{4-t} \in (t, Q)$, such that $\frac{1}{t} - \frac{1}{t'} \leq \frac{1}{p}$, i.e. $\frac{tt'}{t'-t} \geq p$, and $\frac{1}{a} = 1 - \frac{t}{t'}$. Since $\frac{1}{p} + \frac{1}{t} = \frac{1}{2}$, $\frac{t'-t}{t't} p = 1$. Then,

$$\begin{aligned}
\int |\delta q \nabla F(q+\delta q)|^t \, dx &\leq C \left(\int |\delta q|^{at} \, dx\right)^{\frac{1}{a}}\\
&= C \left(\int |\delta q|^{at-p} |\delta q|^p \, dx\right)^{\frac{1}{a}}\\
&\leq C' \left(\left(\int |\delta q|^p \, dx\right)^{\frac{1}{p}}\right)^{\frac{p}{a}}\\
&\leq C' \|\delta q\|_{L^p(\Omega)}^{\frac{t'-t}{t'} p}.
\end{aligned}$$

Therefore,

$$\begin{aligned}
\|F(q) - F(q+\delta q)\|_{W^{1,t}(\Omega)} &\leq C|\delta q \nabla F(q+\delta q)|_{L^t(\Omega)}\\
&= C' \|\delta q\|_{L^p(\Omega)}^{\frac{t'-t}{tt'} p} = C' \|\delta q\|_{L^p(\Omega)},
\end{aligned}$$

completes the third part of this lemma.

$\square$

After considering the continuity of $F(q)$ with respect to L^p norm of q, it follows that F may also be continuous with respect to H^s norm of q.

Lemma 2.18. *Let* $\Omega \subset \mathbb{R}$,

$$X = H^s(\Omega) \quad \textit{for } s \in (1/2, 1),$$
$$Y = H^1(\Omega) \quad \textit{or} \quad L^2(\Omega).$$

Then for $F : U \subset X \to Y$ *defined in* (2.31) *and* $q, q + \delta q \in U$, *there exists* $t \in (2, Q)$ *such that*

$$\|F(q + \delta q) - F(q)\|_{H^1(\Omega)} \leq C\|\delta q\|_{H^s(\Omega)} \tag{2.54}$$
$$\|F(q + \delta q) - F(q)\|_{W^{1,t}(\Omega)} \leq C\|\delta q\|_{H^s(\Omega)}. \tag{2.55}$$

Proof. The second part of Lemma 2.17 states that

$$\|F(q + \delta q) - F(q)\|_{H^1(\Omega)} \leq C_1\|\delta q\|_{L^p(\Omega)}$$

for any $p \in (\frac{2Q}{Q-2}, \infty)$. Based on the third part of Lemma 2.17, there exists a $t \in (2, Q)$, such that

$$\|F(q + \delta q) - F(q)\|_{W^{1,t}(\Omega)} \leq C_2\|\delta q\|_{L^p(\Omega)},$$

for any $p \in (\frac{4Q}{Q-2}, \infty)$.

Based on Theorem 2.8, for any $p \geq 1$,

$$\|\delta q\|_{L^p(\Omega)} \leq C_3\|\delta q\|_{H^s(\Omega)}.$$

Choose $p > \frac{2Q}{Q-2}$, then

$$\|F(q+\delta q) - F(q)\|_{H^1(\Omega)} \leq C_4 \|\delta q\|_{H^s(\Omega)}.$$

Choose $p > \frac{4Q}{Q-2}$, there exists a $t \in (2, Q)$, then

$$\|F(q+\delta q) - F(q)\|_{W^{1,t}(\Omega)} \leq C_5 \|\delta q\|_{H^s(\Omega)}.$$

$\square$

2.2.2.3 Differentiability of the operator

To further investigate the operator F, we consider its differentiability, although the calculation of the derivative of an operator is a bit subtle. In this subsection, we will use $U = H^s(\Omega) \cap \mathcal{S}$, the extended domain of F, as the domain we consider, which is the same one used in Subsection 2.2.2.2. Again, the results here are only valid for $d = 1$, where d is the dimension of Ω.

Take the derivative on both sides of (2.28) and define the operator $F'(q) : H^s(\Omega) \to H_0^1(\Omega)$:

$$\int q \nabla F'(q)\delta q \cdot \nabla v \; dx = -\int \delta q \nabla F(q) \cdot \nabla v \; dx \qquad \forall v \in H_0^1(\Omega), \tag{2.56}$$

where q and $q + \delta q$ are in U.

Some properties about this operator F' will be explored, then that the defined operator is actually the (directional) derivative of F proven. In order to call F' the Fréchet derivative of F, we need to demonstrate properties of the directional derivative $F'(q)\delta q$ for all directions δq in $H^s(\Omega)$. This requires that U contains a ball of finite diameter with respect to the H^s norm. As discussed in Subsection 2.2.1, this is only true for $s > d/2$, i.e., in particular, the following result is only true for $d = 1$.

The operator F' is bounded by the following lemmas with respect to the L^p norm of q for some p, which is similar to the lemma of continuity.

Lemma 2.19. *Let $\Omega \subset \mathbb{R}$ and Q defined in Theorem 2.12, for any $q \in U$,*

1. *for any $p \in (\frac{2Q}{Q-2}, \infty)$, $F'(q) : L^p(\Omega) \to H_0^1(\Omega)$ is bounded;*

2. *for any $p \in (\frac{4Q}{Q-2}, \infty)$, there exists a $t \in (2, Q)$, such that $F'(q) : L^p(\Omega) \to W_0^{1,t}(\Omega)$ is bounded.*

Proof. For the first part, a similar proof is used as in [35]. Choose $v = \nabla F'(q)\delta q$ in the weak formulation (2.56), where

$$\int q \nabla F'(q)\delta q \cdot \nabla v \, dx = -\int \delta q \nabla F(q) \cdot \nabla v \, dx \qquad \forall v \in H_0^1(\Omega),$$

and $t = \frac{2p}{p-2} \in (2, Q)$. Then

$$\begin{aligned}\int_\Omega q|\nabla F'(q)\delta q|^2 \, dx &= -\int_\Omega \delta q \nabla F(q) \cdot \nabla F'(q)\delta q \, dx \\ &\leq \|\delta q\|_{L^p(\Omega)} \|\nabla F(q)\|_{L^t(\Omega)} \|\nabla F'(q)\delta q\|_{L^2(\Omega)} \\ &\leq C\|\delta q\|_{L^p(\Omega)} \|\nabla F'(q)\delta q\|_{L^2(\Omega)}. \qquad \text{(as per Theorem 2.12)}\end{aligned}$$

Thus, $\|\nabla F'(q)\delta q\|_{L^2(\Omega)} \leq C\|\delta q\|_{L^p(\Omega)}$. This finishes the first part.

To prove the second part, apply Theorem 2.12 to (2.56),

$$\|F'(q)\delta q\|_{W^{1,t}(\Omega)} \leq C\|\delta q \nabla F(q)\|_{L^t(\Omega)}. \tag{2.57}$$

Based on a similar estimation of (2.51),

$$\|F'(q)\delta q\|_{W^{1,t}(\Omega)} \leq C\|\delta q\|_{L^p(\Omega)}. \tag{2.58}$$

□

The next lemma bounds the differential operator F' with respect to the H^s norm of q.

Lemma 2.20. *Let $\Omega \subset \mathbb{R}$, $s \in (1/2, 1)$ and Q defined in Theorem 2.12. For any $q \in U$,*

1. *$F'(q) : H^s(\Omega) \to H_0^1(\Omega)$ is bounded.*
2. *There exists a $t \in (2, Q)$, such that $F'(q) : H^s(\Omega) \to W_0^{1,t}(\Omega)$ is bounded.*
3. *For any $p \geq 1$, and any $t \in (2, Q)$ such that for all sequences $\delta q_k \subset U$ where $\|\delta q_k\|_{H^s} \to 0$ as $k \to \infty$, the following is true:*

$$\|F'(q)\delta q_k\|_{W^{1,t}(\Omega)} \to 0. \tag{2.59}$$

Proof. Use a similar proof as in Lemma 2.18 and Lemma 2.19. □

Next, the temporariness from the name of F' can be removed and the operator calculated is proven to be the (directional) derivative of F.

Theorem 2.21. *Let $\Omega \subset \mathbb{R}$, $s \in (1/2, 1)$ and Q defined in Theorem 2.12. Then, the operator $F(q)$ is differentiable, and $F'(q)$ is its derivative, namely for any $q \in U$, and all sequences $\delta q_k \subset U$ where $\|\delta q_k\|_{H^s} \to 0$ as $k \to \infty$, then the following is true:*

$$\frac{\|F(q+\delta q_k) - F(q) - F'(q)\delta q_k\|_{H^1(\Omega)}}{\|\delta q_k\|_{H^s(\Omega)}} \to 0. \tag{2.60}$$

Proof. Recall that in this subsection, we only consider the results when $d = 1$. Thus, U is open in H^s, which provides the directional derivative $F'(q)\delta q$ for all directions in H^s. A similar proof is used as in [35]. Since for any $v \in H_0^1(\Omega)$,

$$\int_\Omega (q + \delta q)\nabla F(q + \delta q) \cdot \nabla v \; dx = \int_\Omega fv \; dx \tag{2.61}$$

$$\int_\Omega q\nabla F(q) \cdot \nabla v \; dx = \int_\Omega fv \; dx \tag{2.62}$$

$$\int q\nabla F'(q)\delta q \cdot \nabla v \; dx = -\int \delta q\nabla F(q) \cdot \nabla v \; dx. \tag{2.63}$$

Let $g = F(q + \delta q) - F(q) - F'(q)\delta q$, then

$$\int (q + \delta q)\nabla g \cdot \nabla v \; dx = -\int \delta q\nabla F'(q)\delta q \cdot \nabla v \; dx. \tag{2.64}$$

Let $v = g$, choose $p \in (\frac{2Q}{Q-2}, \infty)$, and $t = \frac{2p}{p-2}$ then based on Theorems 2.6, 2.7 and 2.8,

$$\begin{aligned}
\int (q + \delta q)|\nabla g|^2 \; dx &= -\int \delta q\nabla F'(q)\delta q \cdot \nabla g \; dx \\
&\leq \|\delta q\|_{L^p(\Omega)}\|\nabla F'(q)\delta q\|_{L^t(\Omega)}\|\nabla g\|_{L^2(\Omega)}, \\
c_0/2\|\nabla g\|_{L^2(\Omega)} &\leq \|\delta q\|_{L^p(\Omega)}\|\nabla F'(q)\delta q\|_{L^t(\Omega)} \\
&\leq \|\delta q\|_{H^s(\Omega)}\|\nabla F'(q)\delta q\|_{L^t(\Omega)}.
\end{aligned}$$

Based on the third part of Lemma 2.20, for any $q \in U$, and all sequences $\delta q_k \subset U$ where $\|\delta q_k\|_{H^s} \to 0$ as $k \to \infty$, then the following is true:

$$\frac{\|F(q + \delta q_k) - F(q) - F'(q)\delta q_k\|_{H^1(\Omega)}}{\|\delta q_k\|_{H^s(\Omega)}} \to 0.$$

□

Furthermore, the operator F' is continuous and, in particular, Lipschitz continuous. The following theorem concerns the Lipschitz condition of the operator $F'(q)$.

Theorem 2.22. *Let $\Omega \subset \mathbb{R}$, $s \in (1/2, 1)$ and Q defined in Theorem 2.12. The operator $F'(q)$ is Lipschitz continuous with respect to $H^s(\Omega)$, namely,*

$$\|F'(q+\delta q) - F'(q)\|_{L(H^s(\Omega), H_0^1(\Omega))} \leq C\|\delta q\|_{H^s(\Omega)} \tag{2.65}$$

for any $q, q+\delta q \in U$.

Proof. A similar proof is used as in [35]. Based on (2.60), for any $v \in H_0^1(\Omega)$, and for any $\chi \in H^s(\Omega)$,

$$\begin{aligned}
\int_\Omega q \nabla F'(q)\chi \cdot \nabla v \, dx &= -\int_\Omega \chi \nabla F(q) \cdot \nabla v \, dx, \\
\int_\Omega (q+\delta q) \nabla F'(q+\delta q)\chi \cdot \nabla v \, dx &= -\int_\Omega \chi \nabla F(q+\delta q) \cdot \nabla v \, dx.
\end{aligned}$$

Then let $w = F'(q+\delta q)\chi - F'(q)\chi$,

$$\int_\Omega q \nabla w \cdot \nabla v \, dx = -\int_\Omega \chi \nabla (F(q+\delta q) - F(q)) \cdot \nabla v \, dx - \int_\Omega \delta q \nabla F'(q+\delta q)\chi \cdot \nabla v \, dx.$$

Let $v = w$, and choose p based on Theorems 2.6, 2.7 and 2.8, and let $t = \frac{2p}{p-2} \in (2, Q)$, then by Hölder's inequality, Lemma 2.18 and Lemma 2.20,

$$\begin{aligned}
\int_\Omega \chi \nabla (F(q+\delta q) - F(q)) \cdot \nabla w \, dx &\leq \|\chi\|_{L^p(\Omega)} \|\nabla (F(q+\delta q) - F(q))\|_{L^t(\Omega)} \|\nabla w\|_{L^2(\Omega)} \\
&\leq \|\chi\|_{L^p(\Omega)} \|\delta q\|_{L^p(\Omega)} \|\nabla w\|_{L^2(\Omega)}.
\end{aligned}$$

$$\int_\Omega \delta q \nabla F'(q+\delta q)\chi \cdot \nabla v \; dx \leq \|\delta q\|_{L^p(\Omega)} \|\nabla F'(q+\delta q)\chi\|_{L^t(\Omega)} \|\nabla w\|_{L^2(\Omega)}$$
$$\leq \|\chi\|_{L^p(\Omega)} \|\delta q\|_{L^p(\Omega)} \|\nabla w\|_{L^2(\Omega)}.$$

Then

$$\|\nabla w\|_{L^2(\Omega)} \leq C\|\chi\|_{H^s(\Omega)} \|\delta q\|_{H^s(\Omega)} \leq C\|\delta q\|_{H^s(\Omega)}. \tag{2.66}$$

This completes the proof. □

The adjoint of $F'(q)$ is defined as shown below (see also [35]):

$$(F'(q))^* : L^2(\Omega) \to H^{-s}(\Omega)$$
$$g \to -\nabla w \cdot \nabla F(q)$$

where w solves the following adjoint problem: $\int_\Omega q \nabla w \cdot \nabla v \; dx = \int_\Omega gv \; dx \quad \forall v \in H_0^1(\Omega)$.

2.2.3 The existence of solutions to the model problem

Now, all the necessary lemmas are provided to prove the existence of solutions for the model problem. The next thing is to demonstrate an existence theorem. Notice that in this subsection, we consider the results that are valid for $d = 1$, 2 or 3, since the theorems in the subsection only require the weak closedness of the operator F.

Theorem 2.23. *Let d be the dimension of the domain Ω.*

$$X = H^s(\Omega) \quad \text{for } 0 < s < 1,$$
$$Y = H^1(\Omega) \quad \text{or} \quad L^2(\Omega).$$

Then a minimizer exists in $D(F)$ for

$$J_\beta(q) = \frac{1}{2}\|F(q) - z\|_Y^2 + \frac{\beta}{2}\|q\|_X^2 \tag{2.67}$$

for $\beta > 0$ a fixed constant.

Proof. By definition, for any $q \in X$, $J_\beta(q) \geq 0$. Therefore, there exists an infimum of the set $J_\beta(q)_{q \in X}$, namely $\inf_{q\in X} J_\beta(q) =: I$.

Let $\epsilon_n = \frac{1}{n}$, there exists a q_n, s.t. $I \leq J_\beta(q_n) < I + \epsilon_n$. When n approaches ∞, $J_\beta(q_n) \to I$.

Also $J_\beta(q_n) \leq J_\beta(q_0) = C$, i.e. $\frac{1}{2}\|F(q_n) - z\|_Y^2 + \frac{\beta}{2}\|q_n\|_X^2 \leq C$, so q_n is uniformly bounded in $X(\Omega)$. Based on Theorem 2.2, since $X = H^s(\Omega)$ is reflexive, there exists a subsequence $\{q_{n_k}\}$, which is weakly convergent.

Without loss of generality, let $n_k = n$, $q_n \rightharpoonup \bar{q}$. By Lemma 2.15, there exists a subsequence $\{F(q_{n_k})\}$ of $\{F(q_n)\}$, such that $F(q_{n_k}) \rightharpoonup \bar{u}$ in Y, and $F(\bar{q}) = \bar{u}$.

The next step is to check $J_\beta(\bar{q}) \leq J_\beta(q) \quad \forall q \in D(F)$.

Based on Theorem 2.1,

$$\|\bar{q}\|_X \leq \liminf_{k\to\infty} \|q_{n_k}\|_X, \tag{2.68}$$

$$\|\bar{u} - z\|_Y \leq \liminf_{k\to\infty} \|u_{n_k} - z\|_Y. \tag{2.69}$$

So,

$$
\begin{aligned}
\frac{1}{2}\|\bar{u} - z\|_Y + \frac{\beta}{2}\|\bar{q}\|_X &\le \liminf_{k\to\infty} \frac{1}{2}\|u_{n_k} - z\|_Y + \frac{\beta}{2}\|q_{n_k}\|_X \\
&= \lim_{k\to\infty} J_\beta(q_{n_k}) \\
&= \inf_{q\in Y} J_\beta(q) \\
&\le \frac{1}{2}\|F(q) - z\|_Y^2 + \frac{\beta}{2}\|q\|_X^2.
\end{aligned}
$$

$\bar{q}$ then is a minimizer of (2.67).

□

The next theorem is the same as the one above except for using $m \in \mathbb{N}$ instead of $s \in (0,1)$.

Theorem 2.24. *Let d be the dimension of the domain Ω.*

$$
\begin{aligned}
X &= H^m(\Omega) \quad \textit{for } m \in \mathbb{N}, \\
Y &= H^1(\Omega) \quad \textit{or} \quad L^2(\Omega).
\end{aligned}
$$

Then a minimizer exists in $D(F)$ for

$$
J_\beta(q) = \frac{1}{2}\|F(q) - z\|_Y^2 + \frac{\beta}{2}\|q\|_X^2
$$

for $\beta > 0$ a fixed constant.

2.2.4 The stability and consistency of the model problem

Although a solution of the model problem exists based on Theorem 2.23, the inverse problem may still be ill-posed due to a lack of stability. If a solution is not stable, a tiny change (resulting from noise or measurement error) in the input, namely the measurement, would lead to a big difference in the output solution. Thus, a natural thing to consider is whether or not a solution is stable [18]. The following theorem that closely follows [22] using H^s seminorm regularization method states the inverse problem (2.67) is stable in terms of the continuous dependence of the solutions on the measurements z^δ. The proof is also similar to the one for existence. In this subsection, the results are also valid for $d = 1$, 2 or 3, since the theorems in the subsection only require the weak closedness of the operator F.

Theorem 2.25. *Let $\beta > 0$ and let $\{z_k\}$ be a sequence where $z_k \to z$, and $\{q_k\} \subset D(F)$ be a sequence of minimizers of* (2.67) *with z replaced by z_k. There exists a subsequence of $\{q_k\}$ that is convergent and the limit of every convergent subsequence is a minimizer of* (2.67).

Proof. Similar to Theorem 2.23, see [22]. □

Recall that the model inverse problem is approximated by a least square minimization method. Even though in this case the method results in an approximated solution that approaches the original solution, it is important to determine whether or not the approximated problem is consistent with the original problem. Hence, the consistency of the problem is also stated (closely following [21], using H^s seminorm regularization method).

Theorem 2.26. *Let $z^\delta \in Y$ with $\|z^\delta - z\| \leq \delta$ and $\beta(\delta)$ be such that $\beta(\delta) \to 0$ and $\frac{\delta^2}{\beta(\delta)} \to 0$ as $\delta \to 0$. Then every sequence $\{q_{\beta_k}^{\delta_k}\} \subset D(F)$, where $\delta_k \to 0$, $\beta_k = \beta(\delta_k)$ and $q_{\beta_k}^{\delta_k}$ is a solution of* (2.67) *with β_k, z^{δ_k} has a convergent subsequence. The limit of every convergent subsequence is a solution of $F(q) = z$. If this solution q^* is unique, then*

$$\lim_{\delta \to 0} q_{\beta(\delta)}^{\delta} = q^*. \tag{2.70}$$

Proof. A similar proof to Theorem 10.3 [21] holds. □

2.2.5 Convergence rates

The model problem has been identified as having a solution that is stable and also consistent with the original solution. It is then logical to question the speed at which that solution can be reached from its initial arbitrary estimate as $\delta \to 0$. The next theorem addresses the convergence rate [39]. Notice that in this subsection, the theorem about convergence rate is only valid for $d = 1$, because the continuity and differentiability of the operator F are required.

Theorem 2.27. *Let $D(F)$ be convex and $\Omega \subset \mathbb{R}$*

$$X = H^s(\Omega) \quad \text{for } s > 1/2,$$
$$Y = H^1(\Omega) \quad \text{or} \quad L^2(\Omega).$$

F is Fréchet differentiable, $u_\delta \in Y$ with $\|u_\delta - z\|_Y \leq \delta$ and q_0 be the solution of $F(q) = z$ with the exact measurement z. If there exists an $\omega \in Y$ such that $q_0 = F'(q_0)^*\omega$ and $L\|\omega\|_Y < 1$, where L is the Lipschitz constant defined in Theorem 2.22, then when $\beta = O(\delta)$ and $\eta = O(\delta^2)$,

$$\|q_\beta^{\delta,\eta} - q_0\| = O(\sqrt{\delta}). \tag{2.71}$$

Proof. $D(F) = X \cap \mathcal{K}$ is convex, where $\mathcal{K} = \{q \in L^\infty(\Omega) : c_0 \leq q \leq c_1 \text{ a.e.}\} \subset U$. Based on Theorem 2.21 and Theorem 2.22, F is Fréchet differentiable on U, thus, F is differentiable on $D(F)$. The same argument as in Theorem 2.4 in [22] is followed. □

Remark. In Theorem 2.27, the operator $F(q)$ needs to be Fréchet differentiable in every direction with the ball $B_\epsilon(q)$, which is the case only when the dimension of the domain Ω is 1. For higher dimensional cases, further investigation is required.

In summary, the first part of this section introduced the useful concepts and theorems related to the theoretical analysis of regularization of inverse problems, including the most significant one – the definition of H^s space and norm. In the second part of this section, the definitions and theorems to the deflection model problem defined in the introduction were applied. Additionally, the existence and stability of solutions, as well as consistency of the problem, were proven. With a few additional conditions, the result of the convergence rate was also determined.

3. NUMERICAL METHODS

The model deflection problem was solved theoretically by proving the existence and stability of solutions in the previous section. Solving the problem numerically is the main topic in this section.

3.1 Optimality conditions

3.1.1 Lagrange multiplier

An analytic solution for the optimization problem presented in the previous sections is not attainable, but a numerical solution can be reached with certain tolerances of error.

In mathematical optimization, the Lagrange multiplier method is used for finding local extrema of a function with constraints. Consider the situation in which the local extrema of an objective function $h(\vec{x})$ are to be determined with a series of constraints $\vec{g}(\vec{x}) = 0$. A new variable $\vec{\lambda}$, the Lagrange multiplier, is introduced to generate the Lagrange function: $\mathcal{L}(\vec{x}, \vec{\lambda}) = h(\vec{x}) + \vec{\lambda} \cdot \vec{g}(\vec{x})$. For each point $\vec{x}^*$ that is a local extremum of h, there exists a $\vec{\lambda}^*$ such that $(\vec{x}^*, \vec{\lambda}^*)$ is a stationary point for the Lagrange function $\mathcal{L}(\vec{x}, \vec{\lambda})$, assuming that certain conditions called "constraint qualifications" are satisfied (see [10,33] for more details). In other words, $\nabla_{\vec{x},\vec{\lambda}} \mathcal{L}(\vec{x}^*, \vec{\lambda}^*) = 0$.

3.1.2 First-order conditions

For problem (1.7), the Lagrange function is defined as follows:

$$\mathcal{L}(u, q, \lambda) = \frac{1}{2}\|u_q - z\|_{L^2}^2 + \frac{\beta}{2}|q|_{H^s(\Omega)}^2 + \int (q\nabla u \cdot \nabla\lambda - f\lambda)dx. \tag{3.1}$$

Here $\frac{1}{2}\|u_q - z\|_{L^2}^2 + \frac{\beta}{2}|q|_{H^s(\Omega)}^2$ is the function to minimize, known as the objective function. The weak formulation $\int(q\nabla u \cdot \nabla\lambda - f\lambda)dx$ is reached from the equality constraint $-\nabla \cdot q\nabla u = f$ by moving f to the left-hand side and taking the L^2 inner product with the Lagrange multiplier λ using integration by parts.

Given (u^*, q^*) as an optimal solution of the problem (1.7), the existence of the Lagrange multiplier λ^* such that (u^*, q^*, λ^*) is a stationary point for the Lagrange function is proven in the first section of [33]. This indicates that the first-order derivative of $\mathcal{L}$ vanishes at that point:

$$\nabla_{u,q,\lambda}\mathcal{L}(u^*, q^*, \lambda^*) = 0. \tag{3.2}$$

This condition along with the original constraints are called the first-order necessary conditions since they involve the first-order derivatives of the objective function and constraints:

$$\begin{aligned}
\frac{\partial\mathcal{L}}{\partial u}(\phi(x))|_{(u^*,q^*,\lambda^*)} &= (u^* - z, \phi) + (q^*\nabla\phi, \nabla\lambda^*) = 0 && \forall\phi,\\
\frac{\partial\mathcal{L}}{\partial q}(\chi(x))|_{(u^*,q^*,\lambda^*)} &= \beta(\nabla^s q^*, \nabla^s\chi) + (\chi\nabla u^*\nabla\lambda^*) = 0 && \forall\chi,\\
\frac{\partial\mathcal{L}}{\partial \lambda}(\psi(x))|_{(u^*,q^*,\lambda^*)} &= (q^*\nabla u^*, \nabla\psi) - (f, \psi) = 0 && \forall\psi.
\end{aligned} \tag{3.3}$$

Here u, λ, ϕ and ψ are in H^1, q and χ are in H^s. These conditions are also called the Karush-Kuhn-Tucker (KKT) conditions.

Remark. From now on, we use x to denote the triple (u, q, λ) for simplicity.

Ito and Kunisch [32] proved similar first-order necessary conditions using slightly different conditions (see also [43, 48]).

3.2 Newton's method

3.2.1 Mathematical setting

Since the analytical solution of (3.2) is not available, a numerical method is required to find an approximate solution of this equation. Newton's method, a powerful algorithm for approximating the zeros of a real function, will be used in this work.

Newton's method, an iterative one, consists of two stages: (1) finding a search direction and, (2) finding a step length to update the approximation. A search direction determines the direction to update the approximation; Newton's method points out a direction to approximate the root. A step length decides the length to reach within a search direction; an ideal step length is 1, because it guarantees a quadratic rate of convergence.

Take a simple one-dimensional real function $h(x)$, for instance. We make an initial guess x_0 about the root, then the method approximates the function $h(x)$ by its tangent line at $x = x_0$. The next step is to find the x-intercept x_1 of that tangent line. Newton's method claims that x_1 is a better approximation to the root of $h(x)$ than x_0. It repeats the steps of finding the tangent line and x-intercept point if necessary. In other words, Newton's method finds a sequence of points that converge to a root of $h(x)$. The procedure is to calculate $x_{n+1} = x_n - \frac{h(x_n)}{h'(x_n)}$ repeatedly until a given accuracy is achieved.

For multi-dimensional functions $\vec{h}(\vec{x})$, Newton's method identifies approximations that approach a root of all the components of $\vec{h}(\vec{x})$, where $\vec{h}$ has as many components as $\vec{x}$. That is to say, Newton's method approximates a root where the tangent surfaces of all the components of $\vec{h}$ have zero intersects.

In solving (3.2), Newton's method is applied to calculate a sequence of $x_k =$

(u_k, q_k, λ_k) to approximate the actual stationary point thereby converging to the true solution as $k \to \infty$. By Newton's method, after k iterations, the next search direction is calculated by

$$\nabla^2_{xx}\mathcal{L}(x_k)\delta x_k = -\nabla_x \mathcal{L}(x_k) \tag{3.4}$$

and the convergence criterion to approximate $\|\nabla_x \mathcal{L}(x_k)\|_2 \to 0$, as $k \to \infty$ is $\|\nabla_x \mathcal{L}(x_k)\|_2 < \epsilon$ for some small ϵ. Here $\nabla^2_{xx}\mathcal{L}$ is also called the Hessian, denoted by H where $H_{ij} = \frac{\partial^2 \mathcal{L}}{\partial x^i \partial x^j}$ assuming x^i and x^j are the ith and jth components of x.

Once the search direction is identified, the next task to consider is the optimal distance to go this direction, also known as the step length. For a quadratic Lagrange function, the full step length 1 is taken ideally. In practice, however, a quadratic Lagrange function may not be available or identify the true behavior of the inverse problem, so adding a line search step to generate a step length will determine how far to go in that search direction. (Line search will be talked about in detail later.) Thus the next iteration is: $x_{k+1} = x_k + \alpha_k \delta x_k$, where α_k is the kth step length.

Computing the second-order derivatives of $\mathcal{L}$ may be challenging when considering non-linear functions. A modification of Newton's method, called the Gauss-Newton method is used for such problems. Unlike Newton's method that requires the calculation of H, the Gauss-Newton method computes a modified Hessian matrix $\bar{H}$ such that second derivatives of the operator F in (2.23) are generally removed. This modified method converges provided that the residual $\|\nabla_x \mathcal{L}\|$ is small (see [11,56,59] for detailed discussions).

In this work, the Gauss-Newton method is used in finding the numerical solutions for the inverse problems because of the simplified calculations (see [42, 51] for comparisons between Newton's method and Gauss-Newton method).

3.2.2 Line search

As mentioned above, a line search determines how far to go in the search direction, i.e. a step length. A merit function is often used to control the step length, which may be related to, but not the same as, the objective function. In an equality-constrained optimization problem, a typical merit function for a line search is always a combination of the objective function and the constraints. An exact step length may be determined by finding a global minimizer of the following function:

$$H(\alpha) = h(x_k + \alpha \delta x_k) \tag{3.5}$$

corresponding to the search direction δx_k, where h is the objective function. However, the computation may be too costly (i.e., time, expense). Hence the goal set up for a line search is not to determine a best step length, but to determine a "good enough" approximate step length. In other words, there is a trade-off. The optimal step length α_k has a significant reduction of the objective function, but may take longer than acceptable to determine. Therefore, the merit function must be chosen carefully.

One merit function, the augmented Lagrange function is chosen for equality-constraint optimization problems (see [23, 24, 48]), namely

$$\phi(x;\mu) = h(x) - \lambda(x)^T g(x) + \frac{1}{2}\mu \|g(x)\|_2^2,$$

where $h(x), g(x)$ represent the objective function and the equality constraints, respectively. Here, $\mu > 0$ is called the penalty parameter that penalizes the measure of the constraints' violations. The accuracy can be improved by increasing the penalty parameter μ. $\lambda(x) = (J(x)J(x)^T)^{-1}J(x)\nabla h(x)$ where $J(x)$ is the Jacobian of the constraint $g(x)$, where $J_{ij} = \frac{\partial g^i}{\partial x_j}$. It turns out that it is complicated to take the derivative of $\phi(x)$ and solve for $\lambda(x)$ because during the calculation, we have to compute third-order tensors, and multiply those with second-order tensors. Resulting from the expensive computation cost, the l_1 merit function (see [48]), which does not require third order tensors during calculation, is used instead. The definition of l_1 merit function is:

$$\phi_1(x;\mu) = h(x) + \mu \sum_i |g^i(x)|,$$

where $h(x)$, $g(x)$ and μ use the same definitions as the augmented Lagrange function.

The choice of l_1 merit function is popular, but it is not differentiable. However, it is directionally differentiable. The directional derivative of ϕ_1 in the direction δx satisfies:

$$D(\phi_1(x_k;\mu);\delta x_k) = \nabla h_k^T \delta x_k - \mu \|g_k\|_1$$

(see [48] for more details). Then, in the line search method, a step length a_k is accepted if the Wolfe condition holds:

$$\phi_1(x_k + \alpha_k \delta x_k;\mu_k) \le \phi_1(x_k,\mu_k) + c_1 \alpha_k D(\phi_1(x_k;\mu);\delta x_k), \quad c_1 \in (0,1).$$

3.3 Discretization

The general structure of utilizing the Lagrange multiplier and Newton's method (or Gauss-Newton method) to solve an optimization problem numerically was introduced in the previous subsections. However, these tools are defined in infinite-dimensional spaces; in order to solve the model deflection problem, a method called discretization is used to reduce the spaces to finite-dimensional ones. More specifically, discretization deals with casting a continuous equation or problem (within infinite-dimensional spaces) into a projection in finite-dimensional spaces.

We use standard continuous finite elements defined on a triangulation for both the state variable u and the Lagrange multiplier λ. For the unknown parameter q, we use piecewise constant shape functions. Using these discrete spaces leads to no difficulties in discretizing the Newton step (3.4) except for the terms including H^s seminorm. We will therefore discuss this term in detail in the following.

3.3.1 Discretization of the H^s seminorm

In Section 2, the H^s seminorm was used as the regularization term and to prove the existence and stability for the membrane problem theoretically. To solve the problem numerically, we need to consider how to actually discretize functions in the H^s space. It turns out that the discretization of $q(x) \in H^s$ is similar to the procedure of discretization in standard Sobolev spaces with integer indices in the way of expressing $q(x)$ with a series of basis functions. That is, choose a set of $\{\chi_i, \forall i\}$ as the basis of a finite dimensional space, and $q_1, q_2, ..., q_N \in \mathbb{R}$ such that $q(x)$ is a linear combination of those $\{\chi_i, \forall i\}$s, i.e. $q(x) = \sum_{i=1}^{N} q_i \chi_i(x)$.

A piecewise constant function would be a good choice for χ_i since this simple function is easy to calculate. We may discretize $|q|^2_{H^s(\Omega)}$ by first writing q as a linear combination of $\{\chi_i, \forall i\}$, namely $q(x) = \displaystyle\sum_{i=1}^{N} q_i \chi_i(x)$.

After expressing the parameter q by a linear combination of all the basis functions, the next step is to compute the discretized H^s seminorm. Even though the basis functions are piecewise constant, the actual calculation of the discrete H^s seminorm for these functions is not straight-forward because of the complicated definition (see Definition 2.14) of fractional Sobolev norm we use.

In the following, let us first calculate expressions for the discrete H^s seminorm and inner products in the 1D case, and then generalize those into the 2D and 3D cases.

The general form for fractional seminorm based on Definition 2.14 is:

$$|u|_{W^{s,p}(\Omega)} := \left(\int_\Omega \int_\Omega \frac{|u(x) - u(y)|^p}{|x - y|^{d+sp}} \ \ dxdy \right)^{\frac{1}{p}},$$

where d is the dimension of Ω.

Let $p = 2$, then the fractional seminorm is:

$$|u|^2_{H^s} = \int_\Omega \int_\Omega \frac{|u(x) - u(y)|^2}{|x - y|^{2s+d}} \, dxdy.$$

The fractional Sobolev space is also a Hilbert space, with the inner product:

$$(u, v)_{H^s(\Omega)} = (u, v)_{L^2(\Omega)} + \int_\Omega \int_\Omega \frac{u(x) - u(y)}{|x - y|^{s+d/2}} \frac{v(x) - v(y)}{|x - y|^{s+d/2}} \, dxdy.$$

Based on this, we can define the following semi-inner product:

$$\langle u, v \rangle_{H^s} := \int_\Omega \int_\Omega \frac{u(x) - u(y)}{|x - y|^{s+d/2}} \frac{v(x) - v(y)}{|x - y|^{s+d/2}} \, dxdy.$$

For 1D case, the seminorm and inner product are defined for piecewise constant shape functions when $s < \frac{1}{2}$. In calculating the discrete H^s seminorm in a unit interval $[0, 1]$, the results are easily extended to any interval by a domain transformation.

Let the domain be $\Omega = [0, 1]$, subdivide it into N subintervals and each interval has the length $h = \frac{1}{N}$. If $u = \chi_{[(i-1)h, ih]}$ and $v = \chi_{[(j-1)h, jh]}$ are defined in $[0, 1]$, then the semi-inner product of u and v in the fractional Sobolev space is

$$\langle u, v \rangle_{H^s} = \int_0^1 \int_0^1 \frac{u(x) - u(y)}{|x - y|^{s+1/2}} \frac{v(x) - v(y)}{|x - y|^{s+1/2}} \, dxdy.$$

Without loss of generality, assume $i < j$, then we can explicitly compute

$$\begin{aligned}
\langle u, v \rangle_{H^s} &= \int_0^1 \int_0^1 \frac{u(x) - u(y)}{|x-y|^{s+1/2}} \frac{v(x) - v(y)}{|x-y|^{s+1/2}} \, dxdy \\
&= 2 \int_{(j-1)h}^{jh} \int_{(i-1)h}^{ih} \frac{-1}{|x-y|^{2s+1}} \, dxdy \\
&= -\frac{h^{1-2s}}{s(1-2s)} \left(2(j-i)^{-2s+1} - (j-i+1)^{-2s+1} - (j-i-1)^{-2s+1} \right). \qquad (3.6)
\end{aligned}$$

The next step is to compute the fractional seminorm of u, which is defined as

$$|u|_{H^s}^2 = \int_0^1 \int_0^1 \frac{|u(x) - u(y)|^2}{|x-y|^{2s+1}} \, dxdy.$$

Again, we can directly compute this norm:

$$\begin{aligned}
|u|_{H^s}^2 &= \int_0^1 \int_0^1 \frac{|u(x) - u(y)|^2}{|x-y|^{2s+1}} \, dxdy \\
&= \int_0^{(i-1)h} \int_{(i-1)h}^{ih} \frac{1}{|x-y|^{2s+1}} \, dxdy + \int_0^{(i-1)h} \int_{(i-1)h}^{ih} \frac{1}{|x-y|^{2s+1}} \, dxdy \\
&\quad + \int_{(i-1)h}^{ih} \int_{ih}^{1} \frac{1}{|x-y|^{2s+1}} \, dxdy + \int_{(i-1)h}^{ih} \int_{ih}^{1} \frac{1}{|x-y|^{2s+1}} \, dxdy \\
&= 2 \int_0^{(i-1)h} \int_{(i-1)h}^{ih} \frac{1}{|x-y|^{2s+1}} \, dxdy + 2 \int_{(i-1)h}^{ih} \int_{ih}^{1} \frac{1}{|x-y|^{2s+1}} \, dxdy. \qquad (3.7)
\end{aligned}$$

In (3.7), we separate $|u|_{H^s}^2$ into two terms depending on whether or not $x - y$ is greater than 0. When $x > y$, we have:

$$\begin{aligned}
\int_0^{(i-1)h} dy \int_{(i-1)h}^{ih} \frac{1}{|x-y|^{2s+1}} \, dx &= \int_0^{(i-1)h} dy \int_{(i-1)h}^{ih} \frac{1}{(x-y)^{2s+1}} \, dx \\
&= \frac{h^{-2s+1}}{2s(1-2s)} \left(1 - i^{-2s+1} + (i-1)^{-2s+1} \right).
\end{aligned}$$

On the other hand, when $x < y$ we have:

$$\int_{ih}^{1} dy \int_{(i-1)h}^{ih} \frac{1}{|x-y|^{2s+1}}\, dx = \int_{ih}^{1} dy \int_{(i-1)h}^{ih} \frac{1}{(y-x)^{2s+1}}\, dx$$
$$= \frac{h^{-2s+1}}{2s(1-2s)} \left(1-(n-i+1)^{-2s+1}+(n-i)^{-2s+1}\right).$$

Thus,

$$|u|_{H^s}^2 = \frac{h^{-2s+1}}{s(1-2s)} \left(2-(n-i+1)^{-2s+1}+(n-i)^{-2s+1}-i^{-2s+1}+(i-1)^{-2s+1}\right). \tag{3.8}$$

A matrix $\bar{R}$ that is associated with the semi-inner product is defined as follows:

$$\bar{R}_{ij} = \begin{cases} -\frac{h^{1-2s}}{s(1-2s)} \left(2((j-i))^{-2s+1}-((j-i+1))^{-2s+1}-((j-i-1))^{-2s+1}\right) & i \neq j \\ \frac{h^{-2s+1}}{s(1-2s)} \left(2-(n-i+1)^{-2s+1}+(n-i)^{-2s+1}-i^{-2s+1}+(i-1)^{-2s+1}\right) & i = j. \end{cases}$$

For this matrix $\bar{R}$, the further the distance between i and j is, namely the larger $|i-j|$ is, the smaller the value of the entry R_{ij} is. Figure 3.1 illustrates this observation.

Since the exact expressions for the entries of $\bar{R}$ are too complicated to use in practice, we will approximate in our numerical computations by

$$|u|_{H^s}^2 \approx \frac{2h^{-2s+1}}{s(1-2s)},$$

and $\langle u, v \rangle_{H^s}$ by

$$\langle u, v \rangle_{H^s} \approx \begin{cases} -\frac{h^{-2s+1}}{s(1-2s)} & |i-j| \leq 1, i \neq j \\ 0 & \text{otherwise.} \end{cases}$$

Notice here that the above approximations about $|u|_{H^s}$ and $\langle u, v \rangle_{H^s}$ correspond

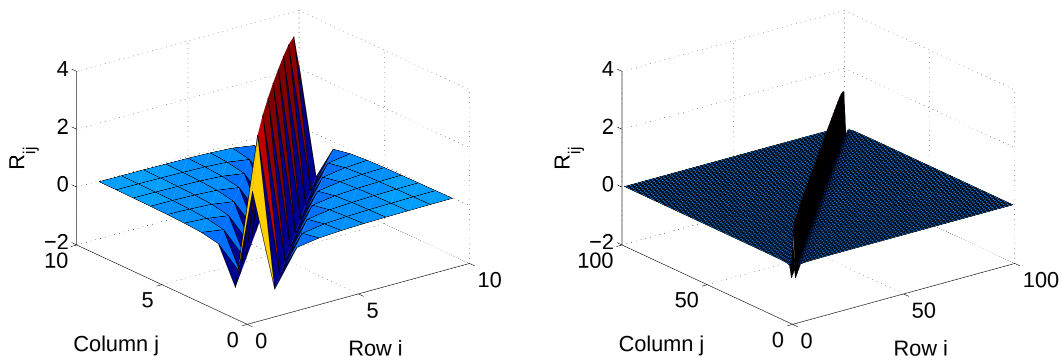

(a) N = 10. (b) N = 100.

Figure 3.1: The elements of the exact matrix, s = 0.25.

to the limit where the domain Ω is large compared to the size of an individual cell.

The decay properties of the off-diagonal elements suggest that we can approximate the full matrix $\bar{R}$ by a matrix that only includes the diagonal and the immediate off-diagonal elements:

$$R = \frac{h^{-2s+1}}{s(1-2s)} \begin{pmatrix} 1 & -1 & & & \\ -1 & 2 & -1 & & \\ & -1 & 2 & & \\ & & & \ddots & \\ & & & -1 & 1 \end{pmatrix}, \qquad R_{ij} = \begin{cases} \frac{2h^{-2s+1}}{s(1-2s)} & i = j \\ -\frac{h^{-2s+1}}{s(1-2s)} & |i-j| \le 1, i \ne j \\ 0 & \text{other} \end{cases} .$$

To determine how well the approximated matrix approaches the exact matrix, we compare the difference between these two matrices. Figure 3.2 shows the difference in two rows between the two matrices, which clearly indicates that the matrix R approximates the exact $\bar{R}$ well. Here N is the number of subintervals.

To quantitatively compare the difference, the L^2 matrix norm (the largest singular

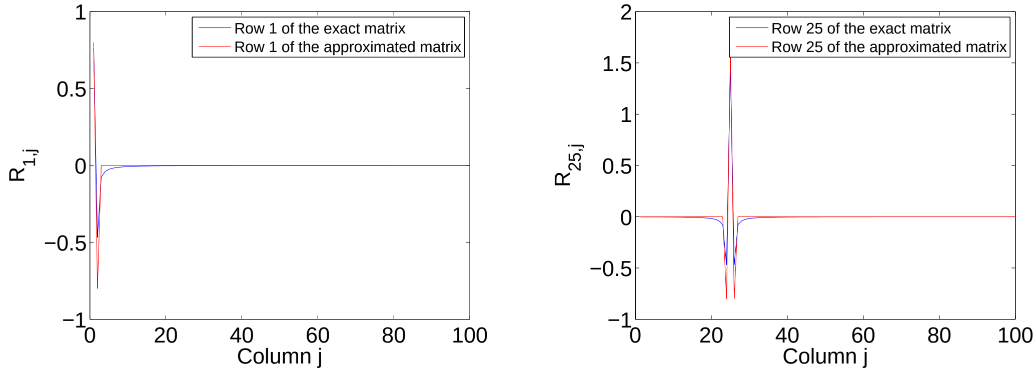

(a) Row 1.

(b) Row 25.

Figure 3.2: Two rows of the exact and approximated matrices ($N = 50, s = 0.25$).

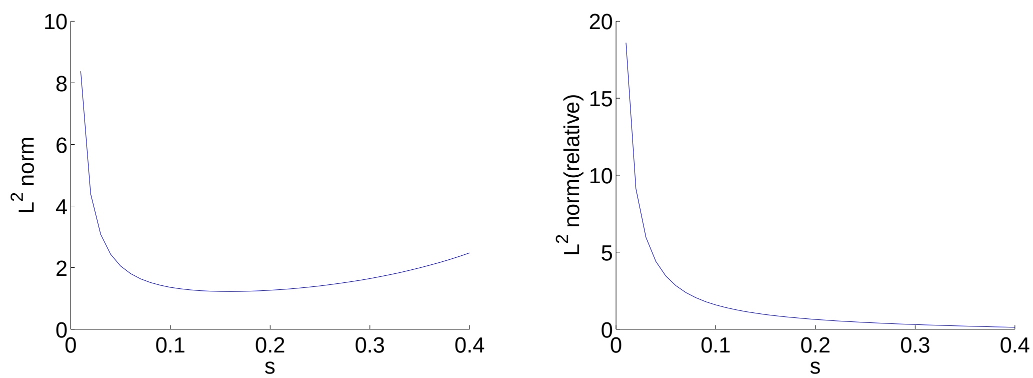

(a) Absolute difference.

(b) Relative difference.

Figure 3.3: L^2 norms of the difference between the approximated and exact matrices ($N = 50$).

value) of the difference between the approximated and exact matrices are shown in Figure 3.3. As depicted from the figures, the relative difference approaches 0 as s goes to 0.5.

After the exact solution for 1D discrete H^s seminorm and inner products has been determined, we may now extend these results to the 2D and 3D cases.

First, let us take a look at a 2D case, namely $d = 2$.

Let the domain be the unit square $\Omega = [0,1]^2$. Unlike the 1D case for which the exact expression for the exact discrete H^s seminorm and inner products can be determined, for the 2D case, only an estimate of the order for the exact seminorm and inner products is possible. The following calculations serve as examples:

If we subdivide the unit square into N by N subintervals, each interval has area h^2, where $h = \frac{1}{N}$. For two cells I and II that are connected only by a corner, without loss of generality, assume the shared corner is the origin. We can then again calculate the following expression directly:

$$\begin{aligned}
\langle u, v\rangle_{H^s} &= -2\int_{II}\int_{I}\frac{1}{|x-y|^{2s+2}}\,dxdy \\
&= -2\int_{II}\int_{I}\left(\big(\underbrace{(x_1-y_1)^2+(x_2-y_2)^2}_{\geq 2|x_1-y_1||x_2-y_2|}\big)^{-s-1}\right)dxdy \\
&\leq -2\int_{-h}^{0}dy_1\int_{0}^{h}dy_2\int_{0}^{h}dx_1\int_{-h}^{0}2^{-s-1}|x_1-y_1|^{-s-1}|x_2-y_2|^{-s-1}\,dx_2 \\
&= -2^{-s}\left(\int_{-h}^{0}dy_1\int_{0}^{h}|x_1-y_1|^{-s-1}\,dx_1\right)\left(\int_{0}^{h}dy_2\int_{-h}^{0}|x_2-y_2|^{-s-1}\,dx_2\right) \\
&= -\frac{2^{-s}}{s(1-s)}h^{2(1-s)}\left(2-2^{-s+1}\right)^2 \\
&\approx O(h^{2-2s}).
\end{aligned}$$

For two cells, I and II, that are adjacent by a segment, without loss of generality, assume one of the shared corners is the origin. Let $a > 0, b > 0, a + b = 2$. We can compute the following expression:

$$
\begin{aligned}
\langle u, v \rangle_{H^s} &= -2 \int_{II} \int_{I} \frac{1}{|x-y|^{2s+2}}\, dxdy \\
&= -2 \int_{II} \int_{I} \left(\frac{1}{\left((x_1 - y_1)^2 + (x_2 - y_2)^2\right)^{s+1}} \right) dxdy \\
&\le C \left(\int_0^h \int_0^h dx_1 dy_1 \, \frac{1}{|x_1 - y_1|^{a(s+1)}} \right) \left(\int_0^h \int_h^{2h} dx_2 dy_2 \, \frac{1}{|x_2 - y_2|^{b(s+1)}} \right) \\
&\le C' h^{2-a(s+1)+2-b(s+1)} \\
&= C' h^{2-2s}.
\end{aligned}
$$

The calculations for two cells that are not adjacent are similar. We may conclude that $\langle u, v \rangle_{H^s}$ is of the order of h^{2-2s}. (For the 1D case, $\langle u, v \rangle_{H^s}$ is of the order of h^{1-2s}). Note that a series of requirements are needed for a, b, s during the computation. First, $a + b = 2$; second, in order for the above integral to have a finite result, we must have $1 - a(s+1) > 0$ and $2 - b(s+1) > 0$. Altogether, we have $s < \frac{1}{2}$. Thus, we may further conclude that the step function is in the H^s space for $s < \frac{1}{2}$ in the 1D and 2D cases.

For the 3D case, we may reach a conjecture that the order of the discrete H^s seminorm and inner products would be h^{3-2s}, with some restrictions on s, based on similar calculations.

In addition, we may consider the constant in front of each element of approximated matrix R as a part of the regularization parameter β.

Based on the analysis here, R_{ij} is approximated as follows: in the 1D case, the matrix is similar to the one that is generated by the finite difference method.

$$R = \frac{1}{h^{2s-1}} \begin{pmatrix} 2 & -1 & & & \\ -1 & 2 & -1 & & \\ & -1 & 2 & & \\ & & \ddots & & \\ & & & -1 & 2 \end{pmatrix}.$$

In d dimensional space, let n be the number of the neighbors of a cell (uniformly refined, without hanging nodes). Then, for each row and each column, there are n number of -1's in the corresponding places. Thus, the matrix is:

$$R = \frac{1}{h^{2s-d}} \begin{pmatrix} n & -1 & -1 & & \\ -1 & n & -1 & -1 & \\ & -1 & n & -1 & \\ & & \ddots & & \\ & & -1 & -1 & n \end{pmatrix}.$$

Therefore, R_{ii} represents $\langle \psi_i, \psi_i \rangle_{H^s}$ and R_{ij} represents $\langle \psi_i, \psi_j \rangle_{H^s}$.

It is important to notice a disparity of the useful range of s in the H^s seminorm between the theoretical results and numerical simulations. In general, s is selected in $(0, 1)$. Theorems of existence, stability and consistence (Theorems 2.23, and 2.26) only require $0 < s < 1$. However, Theorem 2.27 that relates to convergence rates desires a source condition and a Lipschitz differentiable forward operator F that rely on the fact that $s > \frac{d}{Q}$ where d is the dimension of the underlying domain and Q is defined in Theorem 2.12.

On the other hand, the characteristic function $\chi_{[0,1]}$ is in $H^s(\mathbb{R})$ only when $0 \leq$

$s < \frac{1}{2}$ (see, e.g. [58]). This is also true for characteristic functions defined in different intervals. Since H^s spaces with $0 \leq s < \frac{1}{2}$ are meaningful spaces for both theoretical and numerical analysis, these are the ones used in the numerical examples in the next section.

3.3.2 The discretized problem

Newton's method was briefly introduced in Subsection 3.2; that method can be applied to our problem.

Since $\nabla\mathcal{L}$ is the function of which we would like to find roots, the discrete form can be written as $H\ \delta x_k = -b$, where H is the Hessian matrix of Lagrange function $\mathcal{L}$, a square matrix formed by the second-order partial derivatives of the function $\mathcal{L}$ (first order derivative of the target function $\nabla\mathcal{L}$). The gradient of the Lagrange function $\mathcal{L}$ (the target function $\nabla\mathcal{L}$) is b.

In Subsection 3.3.1, how to discretize the H^s seminorm and inner products by expressing those as linear combinations of basis functions was examined. Within the Lagrange function:

$$\mathcal{L}(u, q, \lambda) = \frac{1}{2}\|u_q - z\|_{L^2}^2 + \frac{\beta}{2}|q|_{H^s(\Omega)}^2 + \int (q\nabla u \cdot \nabla\lambda - f\lambda)dx,$$

the notation $\phi_i\ \forall i$ is used as the basis function for u, then $u = \sum_i u_i\phi_i$. Similarly, the notation $\chi_i\ \forall i$ is used as the basis function for λ, and $\lambda = \sum_i \lambda_i\chi_i$.

Hence, in the equation $H\ \delta x_k = -b$ for each Newton step, the search direction, H and b yields a KKT matrix system (see [6] for details):

$$\begin{pmatrix} M & A^T & B^T \\ A & 0 & C \\ B & C^T & \beta R \end{pmatrix} \begin{pmatrix} \delta u_k \\ \delta\lambda_k \\ \delta q_k \end{pmatrix} = \begin{pmatrix} F_1 \\ F_2 \\ F_3 \end{pmatrix}$$

where

$$
\begin{aligned}
M_{ij} &= (\phi_i, \phi_j); & F_{1_i} &= -(u_k - z, \phi_i) - (q_k \nabla \lambda_k, \nabla \phi_i); \\
B_{ij} &= (\psi_i, \nabla \lambda \cdot \nabla \phi_j); & F_{2_i} &= -(q_k \nabla u_k, \nabla \psi_i) + (f, \psi_i); \\
A_{ij} &= (q_k \nabla \psi_i, \nabla \phi_j); & F_{3_i} &= -\beta \left\langle q_k, \chi_i \right\rangle_{H^s} - (\nabla \lambda_k \cdot \nabla u_k, \chi_i); \\
R_{ij} &= \text{defined above}; & C_{ij} &= (\nabla u_k, \chi_j \nabla \psi_i).
\end{aligned} \tag{3.9}
$$

λ would be small, when $(u - z, \phi)$ is small, as a result of the condition that $\forall \phi, \quad \frac{\partial L}{\partial u}(\phi(x)) = (u - z, \phi) + (q \nabla \phi, \nabla \lambda) = 0$. Thus we modify the Newton's method to the Gauss-Newton method as follows:

$$
\begin{pmatrix} M & A^T & 0 \\ A & 0 & C \\ 0 & C^T & \beta R \end{pmatrix} \begin{pmatrix} \delta u_k \\ \delta \lambda_k \\ \delta q_k \end{pmatrix} = \begin{pmatrix} F_1 \\ F_2 \\ F_3 \end{pmatrix},
$$

where M, R, A, C and F are defined in (3.9).

In general, for the contribution of the H^s seminorm to the right-hand side of the KKT system, $F_{3_i} = -\beta(Rq_k)_i - (\nabla \lambda_k \cdot \nabla u_k, \chi_i)$, $\forall i$.

3.3.3 Dealing with bounded unknown parameters

Physical parameters, such as elasticity, are bounded from above and below by considering the extreme cases for the materials. In the model problem, we impose the upper and lower bounds for the unknown parameter, namely $c_0 \leq q(x) \leq c_1$.

One advanced method dealing with inequality properties of $q(x)$ is called active set method. An inequality constraint $g(x) \geq 0$ is active if $g(x) = 0$. The active set contains all the indices of equality constraints and those of active inequality constraints. The basic idea for the active set method is that by iteratively adding and removing the indices of active inequality constraints from the active set, the problem is solved as an equality-constraint optimization problem. The technique used in the numerical computations shown later in this thesis follows the one presented in [6].

3.4 Measurement and noise

In the function $\frac{1}{2}\|u_q - z\|_{L^2}^2 + \frac{\beta}{2}|q|_{H^s}^2 =: J(u, q)$ to minimize, z corresponds to the measurement data that is known before starting Newton's method. The measurement data can be obtained from real world experiments, or calculated with some a priori information.

In the model problem, the synthetic data z is chosen as a higher order finite element solution to the problem $-\nabla \cdot q^*(x)\nabla u(x) = f(x)$ with respect to $u(x)$ plus some noise of level ϵ, where q^* is the exact parameter.

Here, the reason for choosing a higher-order solution for z than u is to avoid an inverse crime (see, e.g. [38]). Inverse crimes involve numerical methods being used to solve an inverse problem that make that problem falsely less ill-posed and with a misleading "better" solution, but does not genuinely reflect reality. These crimes often happen when synthetic data are generated by the same schemes (model, dicretization method, etc.) that are used to solve the inverse problem. For example, if the order of the finite element used in the forward problem in finding z is the same as that of the finite element used in the inverse problem, the solution is deceptively better than it probably would have been had we applied the method to actual measurement data.

A higher-order finite element solution to the problem $-\nabla \cdot q^*(x)\nabla u(x) = f(x)$, namely $u = z$, is not enough to represent real situations. Any real measurement would contain certain levels of noise resulting from many sources. Some level of noise should be added to the synthetic measurement as well to make it as similar to reality as possible. So $Z = (z_i)_{i=1}^N$ (discretized version of the measurement z) becomes

$Z^\epsilon = (z_i + \epsilon_i \max_j |z_j|)$, where ϵ_i is a random variable with Gaussian distribution of mean 0 and variance ϵ. The relative level of noise compared to exact measurements affects the final results we obtain for the inverse problem.

3.5 Multiple experiments

Multiple-measurement results may be available by repeating different experiments, which can be used to reveal different physical situations and increase the accuracy of the reconstruction. In other words, if there are a total of N experiments, there exist N measurements z_l^δ where $l = 1, 2, \ldots, N$. For experiment l, let u^l be the solutions of the equality constraints, which can be called as the state variable, and λ^l be the corresponding Lagrange multiplier where $l = 1, 2, \ldots, N$. We write each of the equality constraints as $A(q, u^l)(\eta) = 0$ where η is within some test space. The optimization problem may be rewritten by the following equation:

$$\begin{aligned} \text{minimize} \quad & \sum_{l=1}^{N} m^l(q, z_l^\delta) + \beta r(q), \\ \text{subject to} \quad & A(q, u^l)(\eta) = 0, \quad \text{where} \quad l = 1, 2, \ldots, N. \end{aligned}$$

In experiment l, $m^k(q, z_l^\delta)$ describes the data misfit between u_k and z_k^δ.

Let $\vec{u} = \{u^1, u^2, \ldots, u^N\}$, $\vec{\lambda} = \{\lambda^1, \lambda^2, \ldots, \lambda^N\}$ and $\vec{x} = \{\vec{u}, q, \vec{\lambda}\}$. The Lagrange function with multiple experiments is almost the same as the one with single experiment, namely

$$\mathcal{L}(\vec{x}) = \sum_{l=1}^{N} m^l(q, z_l^\delta) + \beta r(q) + \sum_{l=1}^{N} A(q, u^l)(\lambda^l). \tag{3.10}$$

The discretization is also similar to the one-experiment case described in Subsection 3.3.1 and follows [6, 7].

The software package that implements multiple experiments is the multiple-experiment parameter estimation library, a library based on deal.II (a Finite Element Differential Equations Analysis Library, see [8]) and consists of three isolated subpackages, namely libparest, me-elliptic and me-tomography. This is a library that targets the numerical solution of inverse problems with multiple experiments. A reconstruction of the parameter can be obtained through one set of observation data; in general, a higher accuracy can be achieved if multiple sets of data may be accessed.

3.6 Summary

In this section, two tools to solve optimization problems, the Lagrange multiplier and Newton's method, were introduced. Then the deflection problem was discretized to set up a linear system. The task is to evaluate the approach described above using concrete numerical examples. We will do so in the next section.

4. NUMERICAL EXAMPLES

The model deflection problem in the introduction is used in this section to test the H^s regularization method, both for 1D and 2D domains. Recall that the original optimization problem is:

$$\min_{u,q} \frac{1}{2}\|u - z\|_{L^2}^2 + \frac{\beta}{2} r(q),$$
$$\text{subject to} - \nabla \cdot q(x) \nabla u(x) = f(x).$$

The corresponding Lagrange function is:

$$\mathcal{L}(u, q, \lambda) = \frac{1}{2}\|u - z\|_{L^2}^2 + \frac{\beta}{2} r(q) + \int (q \nabla u \cdot \nabla \lambda - f\lambda) dx, \tag{4.1}$$

where $r(q)$ can be the H^s seminorm, the L^2 norm or the H^1 seminorm.

In this section, we perform comparisons to quantitatively study the difference of the solutions between the H^s seminorm, L^2 norm, and H^1 seminorm regularization methods. Because we want the reconstruction of the parameter $q(x)$ to be as close as possible to the exact parameter, accuracy is critical. From another aspect, since the use of the regularization parameter β would result in different final solutions, the minimum parameter-reconstruction error for all available βs is also important. Recall that the regularization parameter β serves as a balance between the data misfit $\frac{1}{2}\|u_q - z\|_{L^2}^2$ and the regularization functional $\frac{1}{2} r(q)$. When β is small enough, a suitable solution to minimize the data misfit can be found, yet the regularization does not play its role. When β is too large, the regularization becomes so significant that it overwhelms the data misfit. Then, the problem becomes minimizing the regularization which is not desired.

On the other hand, the reconstruction errors at the same regularization parameter β may not be the same for different norms. Since a larger β provides a greater level of regularization, β that minimizes reconstruction error is expected to be largest for the L^2 norm regularization method that considers only the values of the parameter $q(x)$, smallest for the H^1 seminorm regularization method that considers the values and derivatives of the parameter $q(x)$, and in the middle between the first two for the H^s seminorm regularization method that considers the values of the parameter $q(x)$ as well as the sth derivatives.

It is difficult to seek a suitable regularization parameter, thus the comparisons of minimum reconstruction errors will eliminate the effects resulting from utilizing different βs.

4.1 Reconstructions for continuous parameters

In this subsection, we would like to study the numerical reconstructions for test cases in which we know the exact solution and know the exact parameter is continuous. We will consider both 1D and 2D examples.

4.1.1 1D example

The numerical setup that deals with the 1D exact parameter is defined as follows.

Definition 4.1. Let

$$q(t) = 1 + t^2, \tag{4.2}$$

which is illustrated in Figure 4.1. Here, $f^1(t) = 2$, and $f^l(t) = \pi^2 l^2 \sin(\pi l t)$ for $l = 2, \ldots, N$ are Fourier sine functions, where N represents the number of experiments. Let u^l be a solution of the state equation $-\nabla \cdot q \nabla u^l = f^l$ (see [7]).

Recall that during the discretization, the exact discretized matrix for the H^s seminorm can be achieved for 1D domains. However, the calculation for the exact

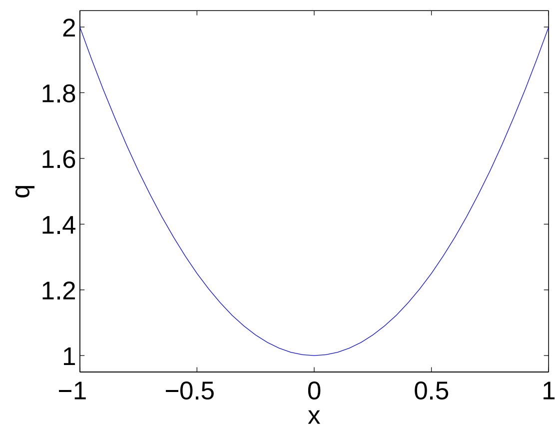

Figure 4.1: The exact 1D continuous parameter.

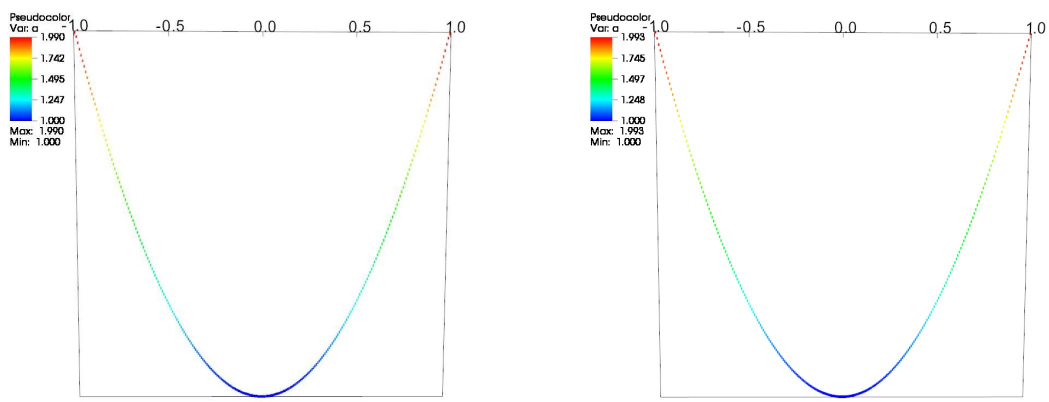

(a) Using exact matrix.

(b) Using approximated matrix.

Figure 4.2: Reconstruction of the 1D continuous parameter q ($N = 8$, $s = 0.5$, $\beta = 10^{-8}$, no additive noise for the measurement z^δ).

discretized matrix is complicated, so it is approximated by a truncated matrix as discussed in Subsection 3.3.1. Figure 4.2 demonstrates that utilizing the truncated matrix results in a good approximation of the parameter q and will be used in further reconstruction by virtue of simplicity.

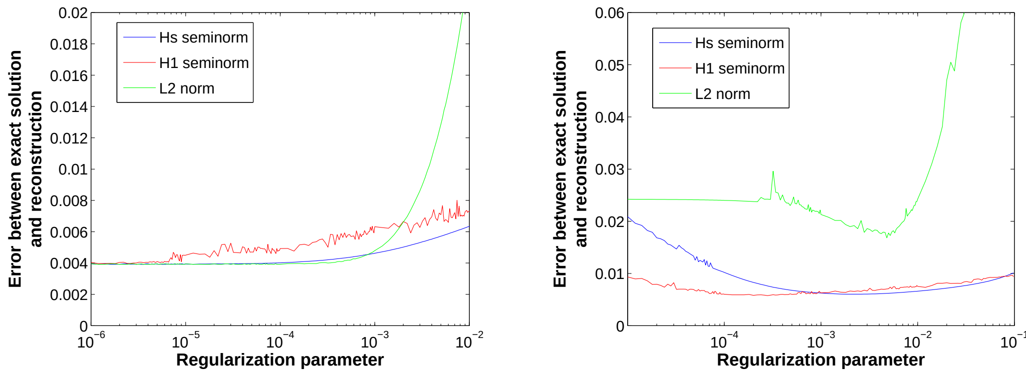

(a) Comparison of different regularization criteria (no additive noise).

(b) Comparison of different regularization criteria (1% additive noise).

Figure 4.3: Reconstruction accuracy of the 1D continuous parameter q ($N = 8$, $s = 0.49$).

Because of the difficulty in finding a suitable regularization parameter, Figure 4.3 illustrates the importance of choosing a suitable β. Each figure indicates a different level of additive noise to the synthetic measurement; inside each figure, each curve shows the value of the function $\|q - q_{\text{exact}}\|$ versus β.

Based on the curves in Figure 4.3a, the three regularization methods do not show a clear preference for the choice of the regularization parameter β regarding the reconstruction accuracy. However, for the ones with additive noise in Figure 4.3b, the minimum error appears when β is a good balance between the data misfit and the regularization functional. Interestingly, considering the reconstruction errors for the 1D continuous parameter q, the H^s seminorm regularization method performs almost as well as the H^1 seminorm regularization method.

4.1.2 2D example

Definition 4.2 provides the numerical setup for reconstructing the 2D exact parameter.

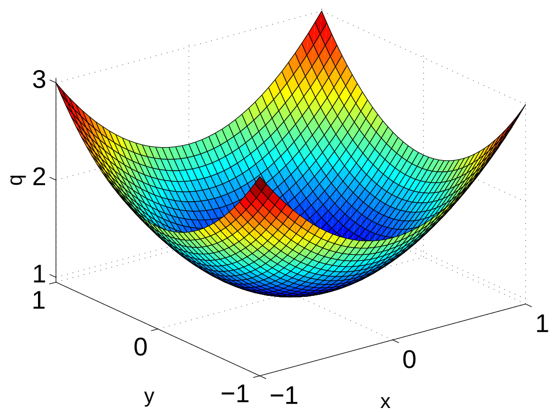

Figure 4.4: The exact 2D continuous parameter.

Definition 4.2. Let $\vec{t} = \{x, y\}$, then

$$q(\vec{t}) = 1 + x^2 + y^2, \tag{4.3}$$

which is illustrated in Figure 4.4. Here, $f^1(\vec{t}) = 4$, and $f^l(\vec{t}) = \pi^2 \vec{k_l}^2 \sin(\pi \vec{k_l} \cdot \vec{t})$ for $l = 2, \ldots, N$ are Fourier sine functions, where N represents the number of experiments and $\vec{k_l}$s are the first N elements of the ordered integer lattice $\{0, 1, 2, \ldots\}^2$ (see [7] for details). Let u^l be a solution of the state equation $-\nabla \cdot q \nabla u^l = f^l$.

The discretized matrix for the H^s seminorm cannot be expressed exactly for 2D domains. An approximate matrix is used in all the reconstructions with the 2D domain here.

Figure 4.5 corresponds to the same comparison as for the 1D example. The information shown in this figure is similar to the 1D example.

4.2 Reconstructions for discontinuous parameters

After examining the reconstruction regarding continuous functions, the next thing to consider is how the new H^s seminorm regularization method acts when handling

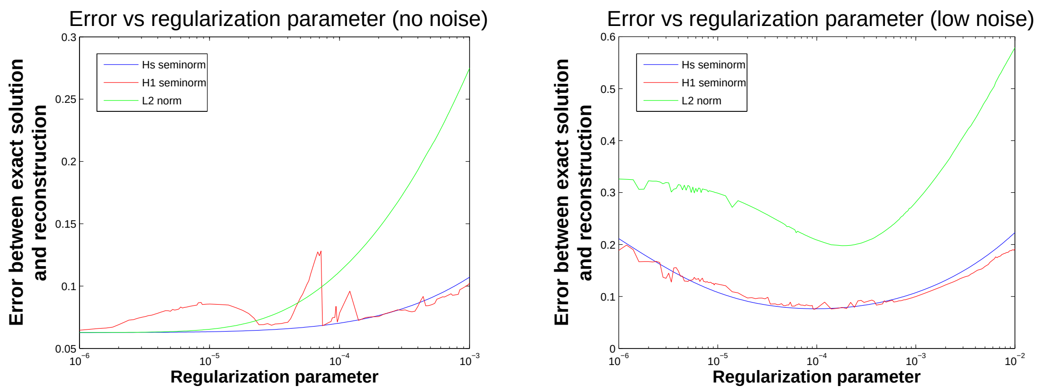

(a) Comparison of different regularization criteria (no additive noise).

(b) Comparison of different regularization criteria (1% additive noise).

Figure 4.5: Reconstruction accuracy of the 2D continuous parameter q ($N = 4$, $s = 0.49$).

the reconstructions of discontinuous functions, the main topic of this subsection. In both one- and two-dimensional cases, the boundary values of $u(x)$ are set as zero Dirichlet boundary conditions.

4.2.1 1D examples

Definition 4.3. Let

$$q(t) = \begin{cases} 1 & |t| < 0.5 \\ 8 & \text{otherwise} \end{cases} \tag{4.4}$$

which is illustrated in Figure 4.6a. Here, $f^1(t) = 2$, and $f^l(t) = \pi^2 l^2 \sin(\pi l t)$ for $l = 2, \ldots, N$ are Fourier sine functions, where N represents the number of experiments (see [7]). Let u^l be a solution of the state equation $-\nabla \cdot q \nabla u^l = f^l$.

Definition 4.4. Let

$$q(t) = \begin{cases} 1 & |t| < 0.5 \\ 1.1 & \text{otherwise} \end{cases} \tag{4.5}$$

which is illustrated in Figure 4.6b. Here, $f^1(t) = 2$, and $f^l(t) = \pi^2 l^2 \sin(\pi l t)$ for $l =$

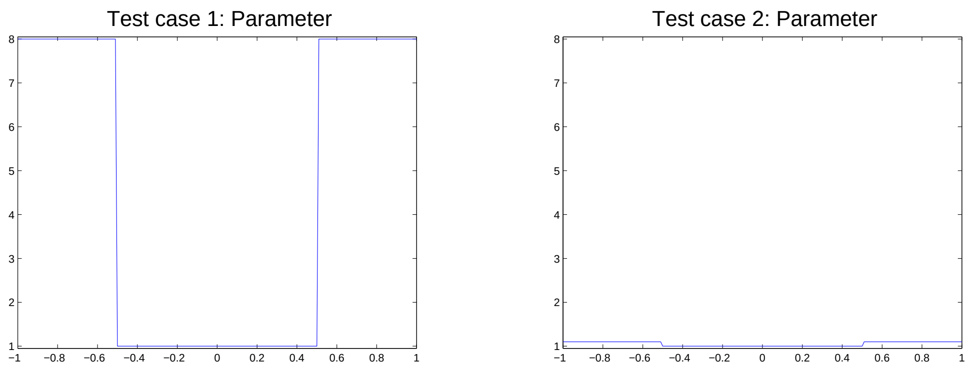

(a) High jump. (b) Low jump.

Figure 4.6: The exact 1D discontinuous parameters q.

$2, \ldots, N$ are Fourier sine functions, where N represents the number of experiments. Let u^l be a solution of the state equation $-\nabla \cdot q\nabla u^l = f^l$.

Similar comparisons between the reconstructions using the truncated and the exact matrices are shown in Figures 4.7 and 4.8. Figure 4.7 again illustrates that the truncated matrices work effectively during the reconstructions and will be used later on for simplicity.

A similar study (Figure 4.9) to Subsection 4.1 is presented to illustrate the relationship between the regularization parameter β and the reconstruction error $\|q - q_{\text{exact}}\|$. For each of the following figures, each curve shows the value of the function $\|q - q_{\text{exact}}\|$ versus β. Since the discussions of these figures here are analogous to the ones for 2D examples, we postpone those to the end of Subsection 4.2.2.

4.2.2 2D examples

In the two-dimensional case, let Ω be $[-1, 1]^2$ and use similar definitions for u and q. The following figures illustrated in Figure 4.10 are sketches of the exact parameters q in 2D examples.

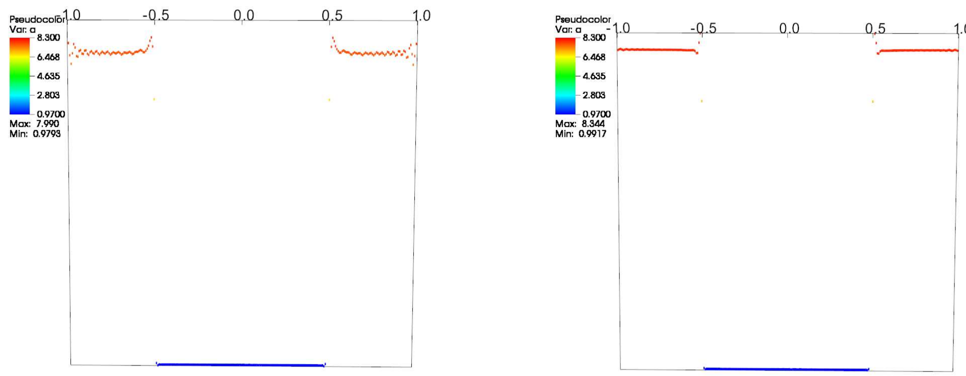

(a) Using exact matrix. (b) Using approximated matrix.

Figure 4.7: Reconstruction of the 1D discontinuous parameter q with high jump ($N = 64$, $s = 0.5$, $\beta = 10^{-6}$, no additive noise for the measurement z^{δ}).

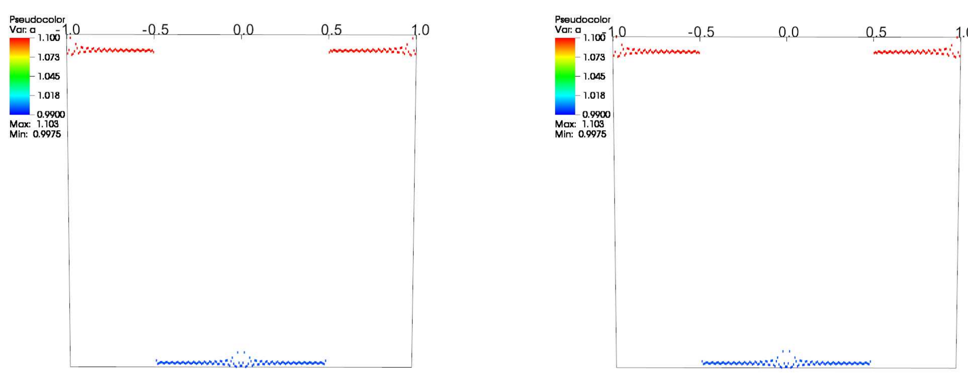

(a) Using exact matrix. (b) Using approximated matrix.

Figure 4.8: Reconstruction of the 1D discontinuous parameter q with low jump ($N = 64$, $s = 0.5$, $\beta = 10^{-5}$, no additive noise for the measurement z^{δ}).

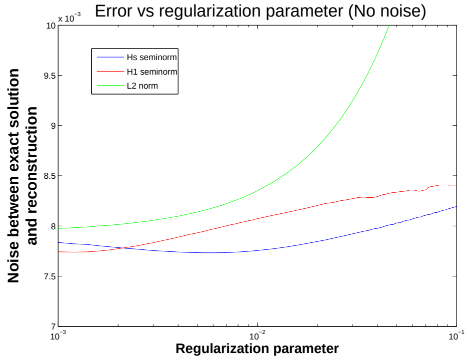

(a) Comparison of different regularization criteria (no additive noise).

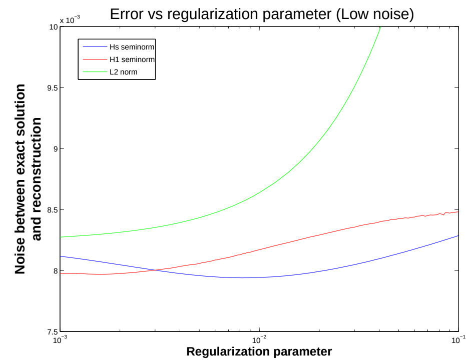

(b) Comparison of different regularization criteria (1% additive noise).

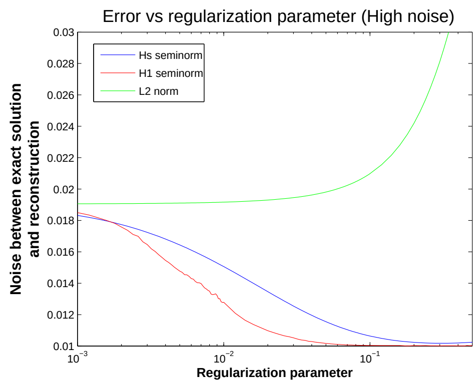

(c) Comparison of different regularization criteria (10% additive noise).

Figure 4.9: Reconstruction accuracy of the 1D discontinuous parameter q with low jump ($N = 64$, $s = 0.49$).

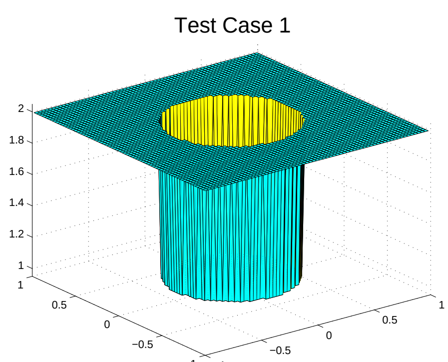

(a) High jump.

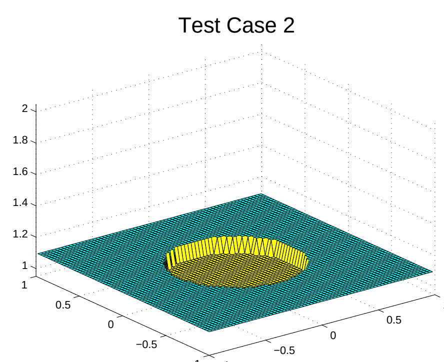

(b) Low jump.

Figure 4.10: The exact parameter of the model problem (2D domain).

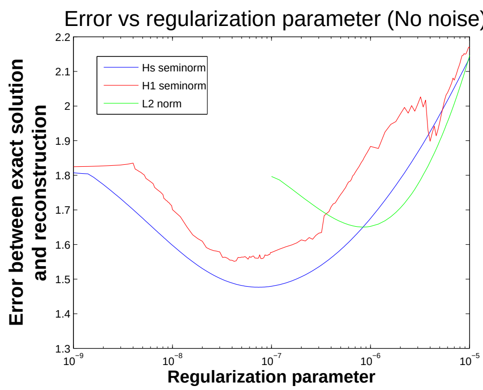

(a) Comparison of different regularization criteria (no additive noise).

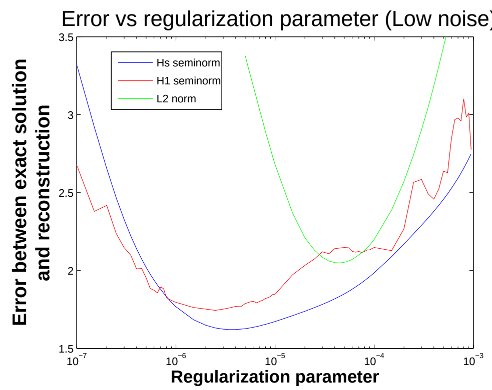

(b) Comparison of different regularization criteria (1% additive noise).

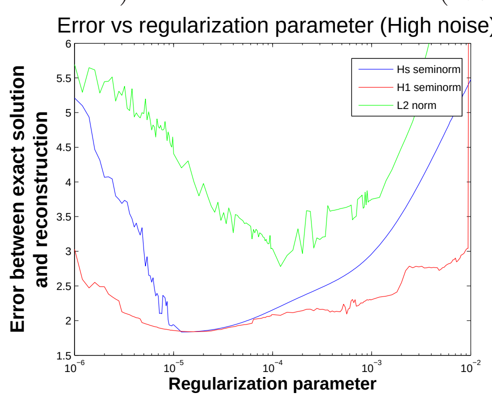

(c) Comparison of different regularization criteria (10% additive noise).

Figure 4.11: Reconstruction accuracy of the 2D discontinuous parameter q with high jump ($N = 8$, $s = 0.49$).

The initial values use $\lambda_0 = 0,\ q_0 = 0.5,\ u_0$ the numerical solution to the Laplace equation as initial values for the Lagrange multiplier, the regularization parameter, and the numerical solution of the PDE constraint, respectively.

As with the 1D examples, the relationships between the regularization parameter β and the reconstruction error $\|q - q_{\text{exact}}\|$ are revealed in Figure 4.11.

After reviewing the figures in Figure 4.11, three important discoveries can be noted here. First, each curve in each figure illustrates an L shape. Either large or small β values would give a larger error for $\|q - q_{\text{exact}}\|$; only those β values in the middle range result in a small error, indicating a good balance between data misfit and the regularization part.

Second, the H^s seminorm regularization method always produces the closest approximation of the exact q, regardless of the noise level. That means the new regularization method truly shows an advancement in solving the inverse problems, at least for this model problem. In other words, the H^s seminorm regularization method is robust for noise level and shows a better approximation for the exact q.

Third, when the noise level increases, all three curves in the figure shift to the right. This indicates that the larger the noise level, the larger the regularization parameter β in order to achieve the lowest error $\|q - q_{\text{exact}}\|$. The largest "best" regularization parameter for 10% additive noise is in the last figure (demonstrated in Figure 4.11c). This phenomenon also reiterates the theme of ill-posedness. Since increasing the noise level makes the problem more ill-posed, increasing the weight of the regularization as well is required so that the "regularized" problem will still be solvable.

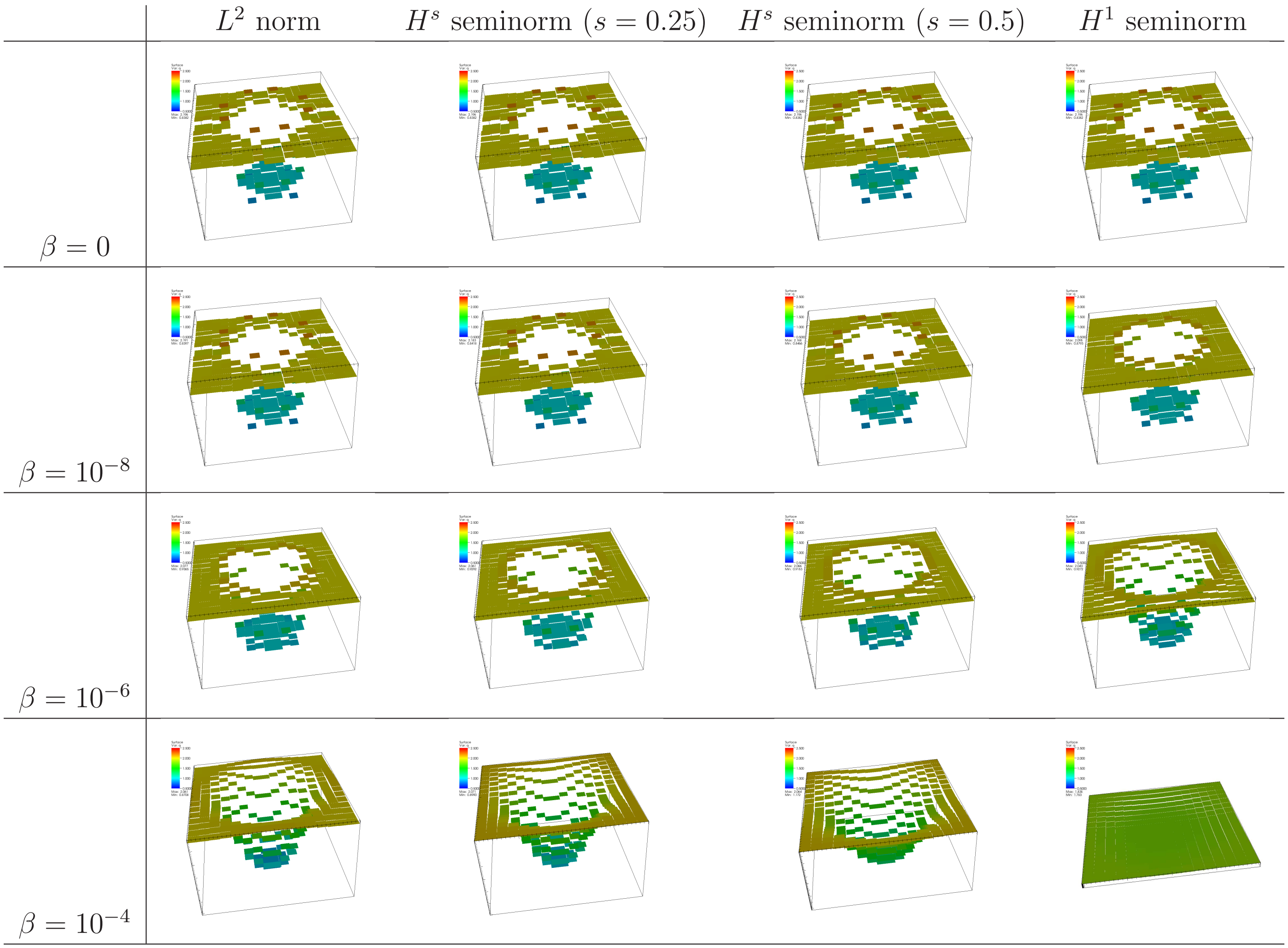

Figure 4.12: Numerical results for H^s seminorm regularization with 4 global refinement steps and no noise.

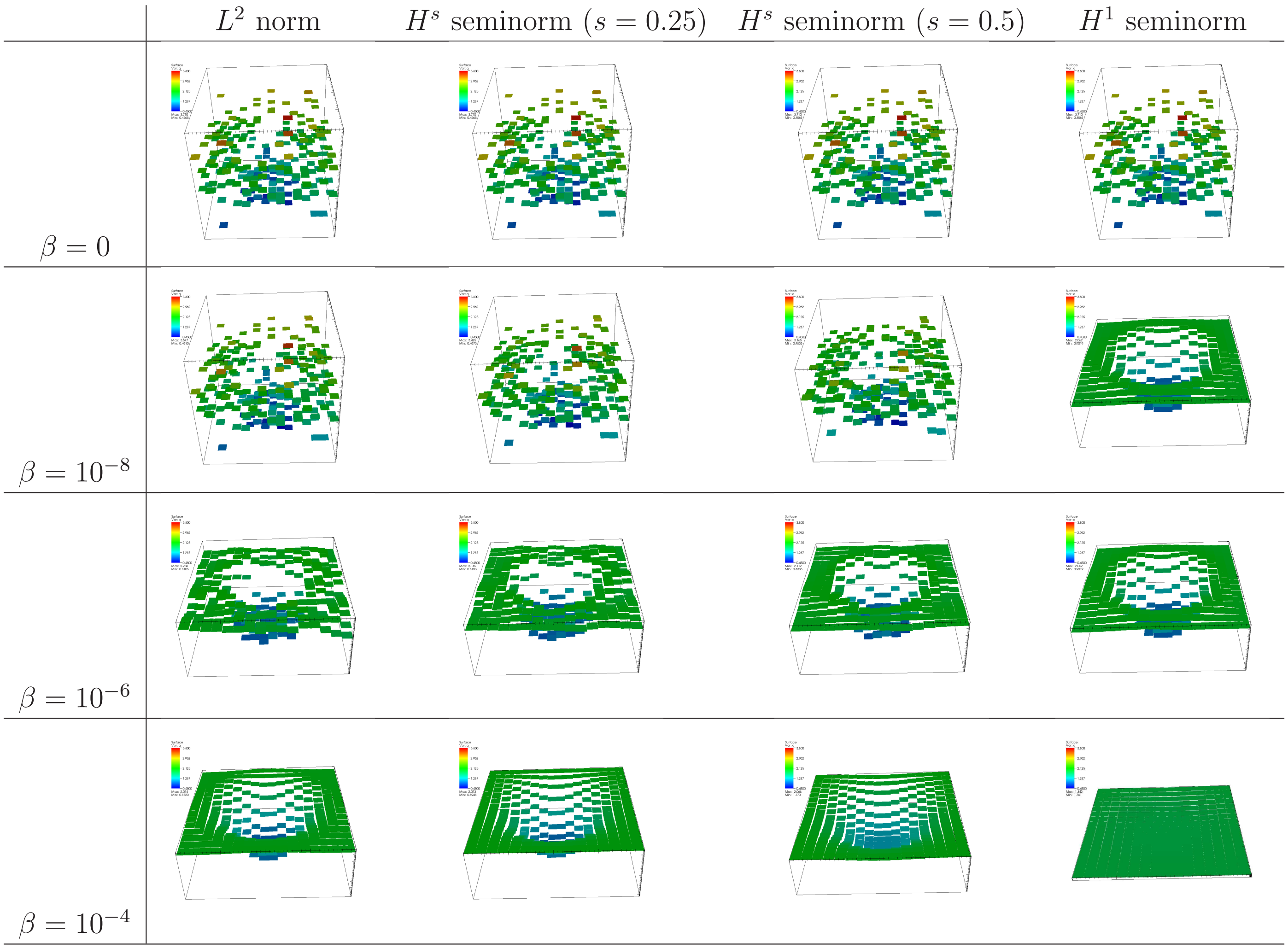

Figure 4.13: Numerical results for H^s seminorm regularization with 4 global refinement steps and 1% additive noise.

	L^2 norm	H^s seminorm $(s = 0.25)$	H^s seminorm $(s = 0.5)$	H^1 seminorm
$\beta = 0$	NA	NA	NA	NA
$\beta = 10^{-8}$	NA	NA	NA	NA
$\beta = 10^{-6}$	NA	NA	NA	NA
$\beta = 10^{-4}$	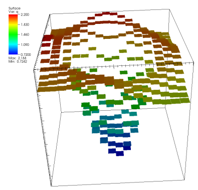	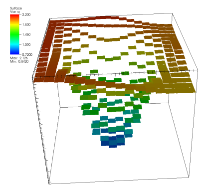	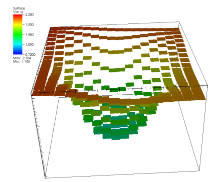	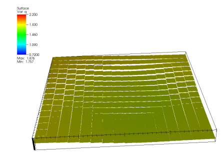

Figure 4.14: Numerical results for H^s seminorm regularization with 4 global refinement steps and 10% additive noise.

	L^2 norm	H^s seminorm $(s = 0.25)$	H^s seminorm $(s = 0.5)$	H^1 seminorm
$\beta = 0$	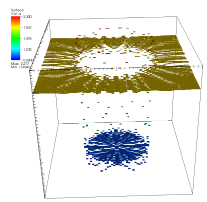	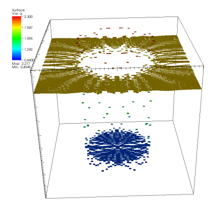	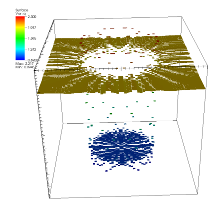	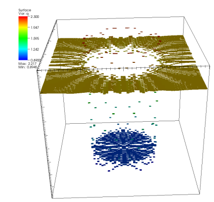
$\beta = 10^{-8}$	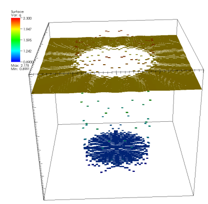	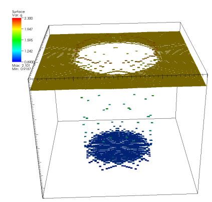	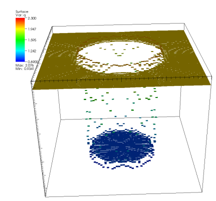	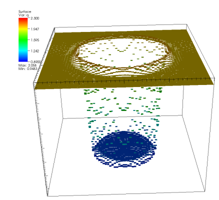
$\beta = 10^{-6}$	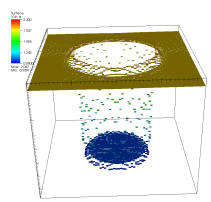	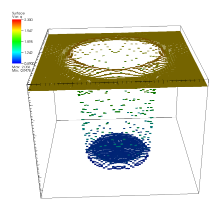	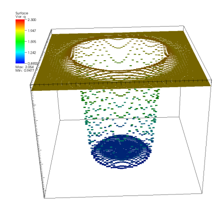	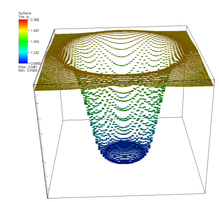
$\beta = 10^{-4}$	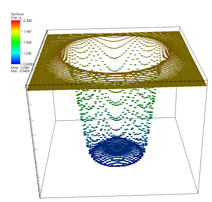	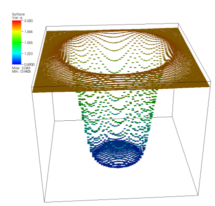	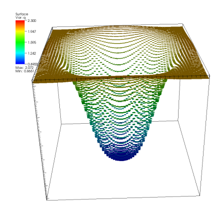	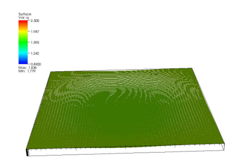

Figure 4.15: Numerical results for H^s seminorm regularization with 6 global refinement steps and no noise.

	L^2 norm	H^s seminorm $(s = 0.25)$	H^s seminorm $(s = 0.5)$	H^1 seminorm
$\beta = 0$	NA	NA	NA	NA
$\beta = 10^{-8}$	NA	NA	NA	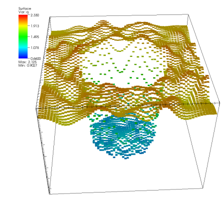
$\beta = 10^{-6}$	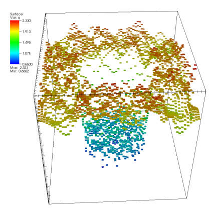	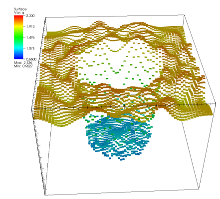	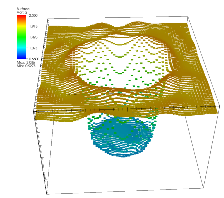	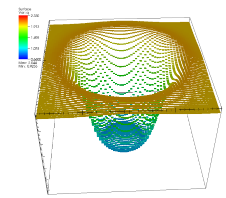
$\beta = 10^{-4}$	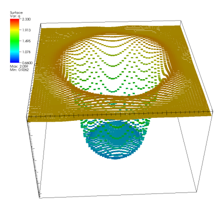	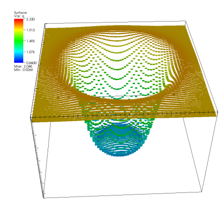	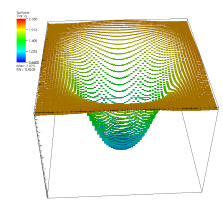	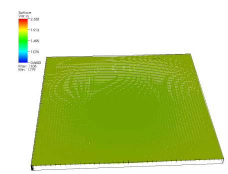

Figure 4.16: Numerical results for H^s seminorm regularization with 6 global refinement steps and 1% additive noise.

	L^2 norm	H^s seminorm $(s = 0.25)$	H^s seminorm $(s = 0.5)$	H^1 seminorm
$\beta = 0$	NA	NA	NA	NA
$\beta = 10^{-8}$	NA	NA	NA	NA
$\beta = 10^{-6}$	NA	NA	NA	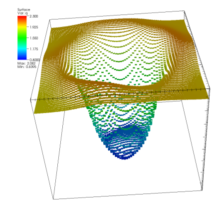
$\beta = 10^{-4}$	NA	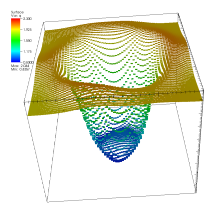	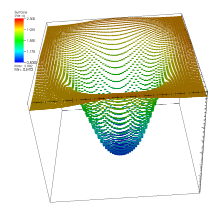	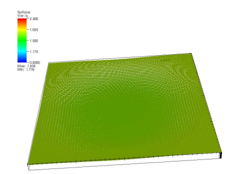

Figure 4.17: Numerical results for H^s seminorm regularization with 6 global refinement steps and 10% additive noise.

Figures 4.12-4.17 show comparisons of the actual reconstructions among the three different regularization methods. Since the model problems are ill-posed, there may be occasions when the numerical approaches can not reach a convergent solution, which is represented by NA (not applicable) in the figures. By examining these reconstructions, it is clear that the regularization parameter β balanced the data misfit with the regularization functional. Once again, the H^s seminorm regularization method produces a better approximation of the exact parameter $q(x)$, while the L^2 norm regularization method creates oscillations, and the H^1 seminorm regularization method creates over-smooth results. Notice that in these figures, we use a H^s seminorm with $s = 0.25$ and 0.5. Although piecewise constant functions only stay in the H^s spaces where $0 < s < 0.5$, the numerous practical results indicate a close similarity between the reconstructed results using $s = 0.49$ and $s = 0.5$. Thus, we also show the reconstructions using $s = 0.5$ in the above figures.

5. AN APPLICATION IN FLUORESCENCE OPTICAL TOMOGRAPHY

A look at tomography offers more practical examples of inverse problem-solving. *Tomography* involves a procedure of imaging using penetrating waves, gathering projection data from multiple directions, and feeding the data into a tomographic reconstruction algorithm processed by a computer.

Tomography can be classified by sources of excitations. For example, computed tomography (CT) scans use X-rays to interrogate the body under investigation; magnetic resonance imaging (MRI) utilizes magnetic fields; seismic tomography exploits seismic waves. Optical tomography uses visible or near infra-red lights to transmit through a target, which has the advantage of less harmful radiation and low-cost devices.

The procedure of diffuse optical tomography (DOT) is as follows: first, it shines near infra-red light from different sources at the target (excitation); second, the light, after reflection, scattering and absorption, is then observed by a sequence of detectors; third, a physical model is used to interpret and reconstruct the underlying structure and properties of the body. The history and methods are reviewed in [12] (see also [5, 29]).

Fluorescence optical tomography has been explored during recent years. The basic idea is to use fluorescent agents to improve the contrast between the healthy and diseased tissues (see e.g. [37, 53], and [54] for an overview).

Fluorescence optical tomography is a nonlinear ill-posed inverse problem. In addition, the reconstruction of a 3D model can be time-consuming. Figure 5.1 is an example of the numerical reconstruction of the concentration of fluorescent dyes based on the H^s seminorm regularization method, where the domain is a 8cm$\times$8cm$\times$4cm

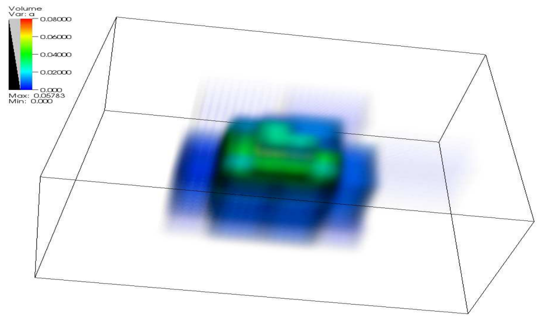

Figure 5.1: Reconstruction of a target using the H^s seminorm regularization method.

rectangular cuboid (see [7] for example); the exact target is a single target placed at 1cm depth underneath the top boundary in the center of the illumination plane. Synthetic measurement data is generated by scanning lines across the surface and measuring the emission field on the boundary. The usage of the H^s regularization method by fluorescence optical tomography is explored in this section.

5.1 Mathematical modeling of the problem

The equality constraints used in fluorescence optical tomography are the state equations derived from the diffusion approximation of the radiative transport equation, which is also known as the *Boltzmann equation* (see [4] for a detailed derivation).

Generally, ω is defined as the frequency with which the incident field is modulated. A fluorescent dye is injected into the body; the intensity field of the light is denoted by a complex-valued function u at the excitation wavelength. The light is scattered, absorbed and then re-emitted for observations, typically with a longer wavelength or a lower energy level, whose intensity field is denoted by another complex-valued v.

Let Ω be the domain of interest and $\partial\Omega$ be the boundary. The propagation of the light during the above procedure can be described as the following state equations:

$$
\begin{aligned}
-\nabla \cdot [D_x \nabla u] + k_x u &= 0, \\
-\nabla \cdot [D_m \nabla v] + k_m v &= b_{xm} u,
\end{aligned}
\tag{5.1}
$$

where the subscript x represents the excitation, and m the emission. The coefficients in (5.1) are:

$$
\begin{aligned}
D_x &= \frac{1}{3(\mu_{axi} + \mu_{axf} + \mu'_{sx})}, & D_m &= \frac{1}{3(\mu_{ami} + \mu_{amf} + \mu'_{sm})}, \\
k_x &= \frac{i\omega}{c} + \mu_{axi} + \mu_{axf}, & k_m &= \frac{i\omega}{c} + \mu_{ami} + \mu_{amf}, \\
b_{xm} &= \frac{\phi \mu_{axf}}{1 + i\omega\tau},
\end{aligned}
$$

where Ds are the diffusion coefficients and c is the speed of light. Assume μ_{axi} and μ_{ami} are the absorption coefficients of the endogenous chromophores; μ_{axf} and μ_{amf} are the absorption coefficients of the exogenous fluorophore; μ'_{sx} and μ'_{sm} are the reduced scattering coefficients. Also assume ϕ stands for the fluorophore quantum efficiency, and τ represents the half-life of the fluorophore. The boundary conditions are of Robin-type. (See [7] for details.)

$$
\begin{aligned}
2D_x \frac{\partial u}{\partial n} + \gamma u + S &= 0, \\
2D_m \frac{\partial v}{\partial n} + \gamma v &= 0,
\end{aligned}
\tag{5.2}
$$

where S defined on the boundary $\partial\Omega$ denotes the excitation boundary source, n is the outward normal to the surface and γ is a reflectivity constant (see [37]).

The unknown coefficient in this work is the absorption coefficient μ_{axf}; other coefficients are considered given. In other words, the purpose of solving the fluorescence optical tomography problem here is to reconstruct μ_{axf} based on the measurements of the emissions on the boundary of the target and their relationships (5.1) and (5.2). To indicate the special role of this coefficient, we will henceforth denote $q := \mu_{axf}$.

Let us denote $\tau = \{\eta, \theta\} \in H^1(\Omega)$ as test functions, then the weak formulation of the state equations can be expressed as (see [7]):

$$
\begin{aligned}
A(q; u, v)(\tau) &= (D_x \nabla u, \nabla \eta)_\Omega + (k_x u, \eta)_\Omega + \frac{\gamma}{2}(u, \eta)_{\partial\Omega} + \frac{1}{2}(S, \eta)_{\partial\Omega} \\
&+ (D_m \nabla v, \nabla \theta)_\Omega + (k_m v, \theta)_\Omega + \frac{\gamma}{2}(v, \theta)_{\partial\Omega} - (b_{xm} u, \theta)_\Omega = 0.
\end{aligned}
$$

The corresponding optimization problem can also be denoted by (1.4). However, since the measurements are only available on the boundary, the data misfit $m(q, z^\delta)$ in (1.4) is a distance between the states and measurements on the boundary instead of the entire domain. The measurements z can be generated using multiple sources, which results in the following optimization problem (see [7] for details):

$$
\begin{aligned}
\text{minimize} \quad & \sum_{l=1}^{N} m^l(q, z_l^\delta) + \beta r(q), \\
\text{subject to} \quad & A(q; u^l, v^l)(\tau) = 0, \qquad l = 1, \ldots, N.
\end{aligned}
$$

In experiment l, z_l^δ represent the measurement value; $m^l(q, z_l^\delta)$ describes the distance between predicted values of v and the measurements z on the boundary $\partial\Omega$. $A(q; u^l, v^l)(\tau)$ denotes the equality constraints (5.1). We use $m^l(q, z_l^\delta) = \frac{1}{2}\|v^l - z_l^\delta\|_{L^2(\partial\Omega)}$ and $r(q) = \frac{1}{2}|q|_{H^s(\Omega)}$.

A similar Lagrange function to the nondestructive evaluation example can be reached:

$$
\mathcal{L}(v, q, \lambda) = \sum_{l=1}^{N} \frac{1}{2}\|v^l - z_l^\delta\|_{L^2(\partial\Omega)} + \frac{1}{2}|q|_{H^s(\Omega)} + \sum_{l=1}^{N} A(q; u^l, v^l)(\lambda^l). \tag{5.3}
$$

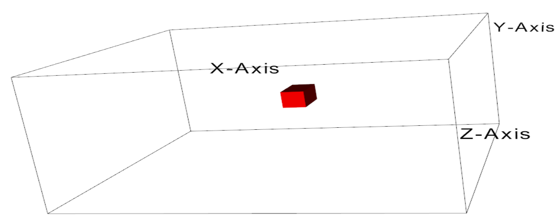

Figure 5.2: Model problem.

The Gauss-Newton method is utilized to find the stationary point. More details are discussed in [7, 9, 36].

5.2 Numerical examples

In this subsection, a model problem with synthetic measurement data is presented for image reconstructions discussed in Subsection 5.1. In this numerical example, the domain is a 8cm×8cm×4cm rectangular cuboid; a 1cm^3 cube is placed at 1cm depth underneath the top boundary in the center of the illumination plane. The synthetic measurement data is generated by scanning lines across the surface and measuring the emission field on the boundary (see Figure 5.2).

Figures 5.3, 5.4 show comparisons of the actual reconstructions of the tomography problem among the three different regularization methods. By examining these reconstructions, the regularization parameter β made a trade-off between the data misfit and the regularization functional. Comparing Figure 5.3 with Figure 5.4, the regularization parameter used in the later figure is larger than the former one, because increased noise levels result in an ill-posed situation that requires stronger regularization. The H^s seminorm regularization method produces a better approximation of the exact parameter $q(x)$ for some of the regularization parameters, while the L^2

norm regularization method creates oscillations and the H^1 seminorm regularization method made the results over-smooth. Finding a better regularization parameter β for each of the regularization methods is subject matter for further study and is beyond the scope of this work.

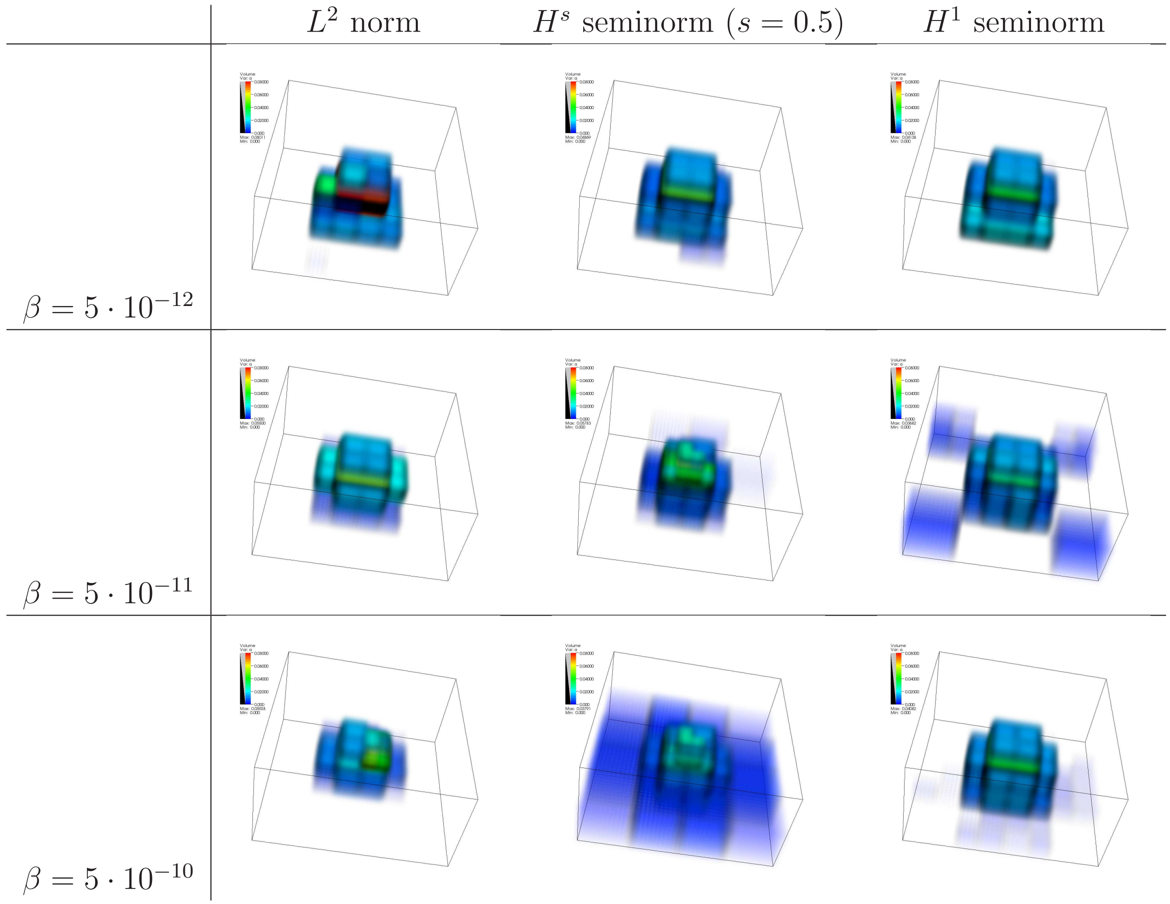

Figure 5.3: Volume rendering of reconstructions for single-target fluorescence optical tomography problem (no additive noise).

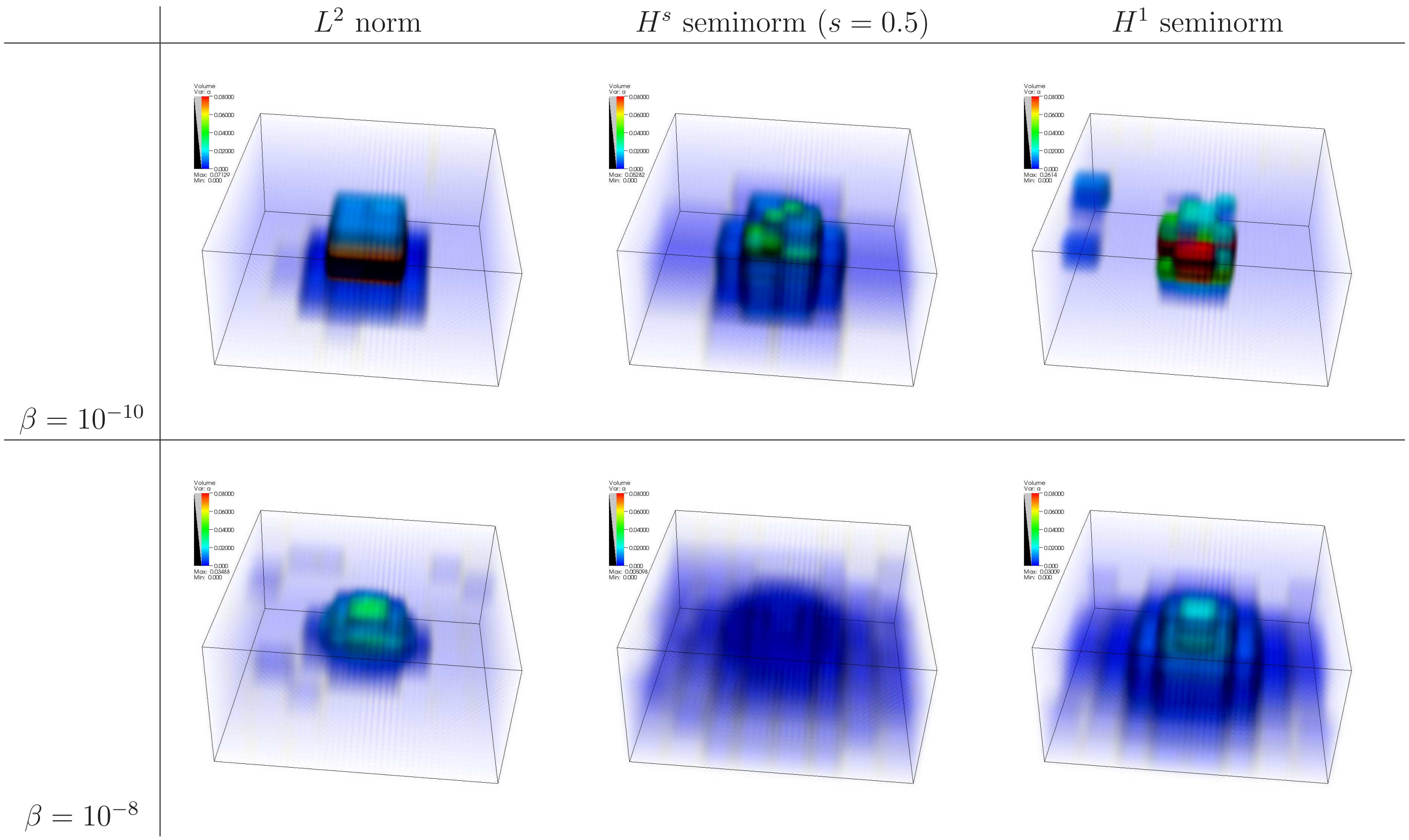

Figure 5.4: Volume rendering of reconstructions for single-target fluorescence optical tomography problem (1% additive noise).

6. CONCLUSIONS

An inverse problem involves obtaining unknown parameters based on information collected by observations. Typically, regularization is imposed in order to solve an inverse problem because of the ill-posedness. In this dissertation, we have studied and implemented a novel H^s seminorm regularization method for inverse problems. This method relies on the evaluation of the seminorms of an intermediary Hilbert space, namely H^s space, that stays between L^2 and H^1. We used this method to minimize the undesirable aspects of the existing L^2 and H^1 regularization methods. In addition, the H^s seminorm regularization method allows for discontinuous reconstructions while stabilizing oscillations.

In Section 2, we conducted a theoretical analysis for the H^s seminorm regularization method corresponding to a nondestructive evaluation model problem. We first introduced the definitions for H^s spaces and norms, along with some useful theorems, and then we studied and proved some properties for the operator defined in (2.31). Based on these properties, we proved the existence and stability of the solution for the model problem. Furthermore, we proved convergence and achieved a convergence rate of $O(\sqrt{\delta})$ where δ is the noise level provided some conditions when the considered domain is 1D.

In Section 3, we presented the methods to discretize the model problem, for example, Lagrange multiplier and Newton's method. In particular, we included an approximated discretization of the H^s seminorm that can be applied to 1D, 2D or 3D examples using piecewise constant functions. The discretization of the H^s seminorm using higher order polynomials is still under development due to the complicated definition of the H^s seminorm.

In Section 4, we provided numerical results using the H^s seminorm regularization method, namely the reconstructions of both continuous and discontinuous parameters from synthetic data and a comparison of these solutions to the ones based on existing L^2 and H^1 regularization methods. The numerical results indicate the robustness of the method. Moreover, the analysis in this section suggests that the H^s seminorm regularization method produces the closest approximation of the exact q than the L^2 norm and H^1 seminorm regularization methods.

In Section 5, we applied our regularization method to another model problem – a fluorescence optical tomography problem. We studied the mathematical modeling and some numerical results. A further analysis and numerical investigation of this real world problem is left for future work.

REFERENCES

[1] R. Acar and C.R. Vogel. Analysis of bounded variation penalty methods for ill-posed problems. *Inverse Problems*, 10(6):1217, 1994.

[2] R.A. Adams and J.J.F. Fournier. *Sobolev Spaces*, volume 140. Academic Press, Amsterdam, The Netherlands, 2003.

[3] M. Allmaras and W. Bangerth et al. Estimating parameters in physical models through bayesian inversion: A complete example. *SIAM Review*, 55:149–167, 2013.

[4] S.R. Arridge. Optical tomography in medical imaging. *Inverse Problems*, 15(2):R41, 1999.

[5] S.R. Arridge and J.C. Hebden. Optical imaging in medicine: II. modelling and reconstruction. *Physics in Medicine and Biology*, 42(5):841, 1997.

[6] W. Bangerth. *Adaptive Finite Element Methods for the Identification of Distributed Parameters in Partial Differential Equations*. PhD thesis, University of Heidelberg, Heidelberg, Germany, 2002.

[7] W. Bangerth. A framework for the adaptive finite element solution of large inverse problems. *SIAM Journal on Scientific Computing*, 30:2965–2989, 2008.

[8] W. Bangerth, R. Hartmann, and G. Kanschat. deal.II – a general purpose object oriented finite element library. *ACM Transactions on Mathematical Software (TOMS)*, 33(4):24, 2007.

[9] W. Bangerth and A. Joshi. Adaptive finite element methods for the solution of inverse problems in optical tomography. *Inverse Problems*, 24:034011/1–22, 2008.

[10] H.T. Banks and K. Kunisch. *Estimation Techniques for Distributed Parameter Systems*. Birkhauser Boston, Harrisonburg, VA, 1989.

[11] B. Blaschke, A. Neubauer, and O. Scherzer. On convergence rates for the iteratively regularized Gauss-Newton method. *IMA Journal of Numerical Analysis*, 17(3):421–436, 1997.

[12] D. Boas, D. Brooks, E. Miller, C. DiMarzio, M. Kilmer, R. Gaudette, and Q. Zhang. Imaging the body with diffuse optical tomography. *Signal Processing Magazine, IEEE*, 18(6):57–75, 2001.

[13] L. Cesari and P. Kaiser. Closed operators and existence theorems in multidimensional problems of the calculus of variations. *Bulletin of the American Mathematical Society*, 80(3):473–478, 1974.

[14] T. Chan and X. Tai. Level set and total variation regularization for elliptic inverse problems with discontinuous coefficients. *Journal of Computational Physics*, 193(1):40–66, 2004.

[15] T.F. Chan, G.H. Golub, and P. Mulet. A nonlinear primal-dual method for total variation-based image restoration. *Lecture Notes in Control and Information Sciences, ICAOS '96*, 219/1996:241–252, 1996.

[16] C. Clason, B. Jin, and K. Kunisch. A duality-based splitting method for L1-TV image restoration with automatic regularization parameter choice. *SIAM Journal on Scientific Computing*, 32(3):1484–1505, 2010.

[17] C. Clason, B. Jin, and K. Kunisch. A semismooth Newton method for L1 data fitting with automatic choice of regularization parameters and noise calibration. *SIAM Journal on Imaging Sciences*, 3(2):199–231, 2010.

[18] F. Colonius and K. Kunisch. Output least squares stability in elliptic systems. *Applied Mathematics and Optimization*, 19(1):33–63, 1989.

[19] B. Dacorogna. *Introduction to the Calculus of Variations*. Imperial College Press, London, UK, 2004.

[20] F. Demengel and G. Demengel. *Functional Spaces for the Theory of Elliptic Partial Differential Equations*. Springer, London, UK, 2012.

[21] H.W. Engl, M. Hanke, and A. Neubauer. *Regularization of Inverse Problems*, volume 375. Springer, Dordrecht, The Netherlands, 1996.

[22] H.W. Engl, K. Kunisch, and A. Neubauer. Convergence rates for Tikhonov regularisation of non-linear ill-posed problems. *Inverse Problems*, 5(4):523, 1989.

[23] R. Fletcher. A class of methods for nonlinear programming with termination and convergence properties. *Integer and Nonlinear Programming*, pages 157–173, 1970.

[24] P.E. Gill, W. Murray, M.A. Saunders, and M.H. Wright. Some Theoretical Properties of an Augmented Lagrangian Merit Function. Technical report, DTIC Document, 1986.

[25] G.H. Golub, P.C. Hansen, and D.P. O'Leary. Tikhonov regularization and total least squares. *SIAM Journal on Matrix Analysis and Applications*, 21:185–194, 1999.

[26] J. Hadamard. *Lectures on Cauchy's problem: In linear partial differential equations*. Courier Dover Publications, Mineloa, NY, 2003.

[27] P.C. Hansen. Numerical tools for analysis and solution of Fredholm integral equations of the first kind. *Inverse Problems*, 8(6):849, 1992.

[28] P.C. Hansen and D.P. O'Leary. The use of the L-curve in the regularization of discrete ill-posed problems. *SIAM Journal on Scientific Computing*, 14(6):1487–1503, 1993.

[29] J.C. Hebden, S.R. Arridge, and D.T. Delpy. Optical imaging in medicine: I. experimental techniques. *Physics in Medicine and Biology*, 42(5):825, 1997.

[30] F. Herrmann and G. Hennenfent. Non-parametric seismic data recovery with curvelet frames. *Geophysical Journal International*, 173(1):233–248, 2008.

[31] K. Ito, B. Jin, and J. Zou. A new choice rule for regularization parameters in Tikhonov regularization. *Applicable Analysis*, 90(10):1521–1544, 2011.

[32] K. Ito and K. Kunisch. The augmented Lagrangian method for parameter estimation in elliptic systems. *SIAM Journal on Control and Optimization*, 28(1):113–136, 1990.

[33] K. Ito and K. Kunisch. *Lagrange Multiplier Approach to Variational Problems and Applications*, volume 15. SIAM, Philadelphia, PA, 2008.

[34] B. Jafarpour and D.B. McLaughlin. Reservoir characterization with the discrete cosine transform. *SPE Journal*, 14(1):182–201, 2009.

[35] B. Jin and P. Maass. An analysis of electrical impedance tomography with applications to Tikhonov regularization. *ESAIM: Control, Optimisation and Calculus of Variations*, 1(1), 2011.

[36] A. Joshi, W. Bangerth, and E.M. Sevick-Muraca. Adaptive finite element based tomography for fluorescence optical imaging in tissue. *Optics Express*, 12(22):5402–5417, 2004.

[37] A. Joshi, W. Bangerth, and E.M. Sevick-Muraca. Non-contact fluorescence optical tomography with scanning patterned illumination. *Optics Express*, 14:6516–6534, 2006.

[38] J. Kaipio and E. Somersalo. *Statistical and Computational Inverse Problems*, volume 160. Springer, New York, NY, 2005.

[39] K. Kunisch and G. Chavent. Convergence of Tikhonov regularization for constrained ill-posed inverse problems. *Inverse Problems*, 10(1), 1994.

[40] G. Leoni. *A First Course in Sobolev Spaces*, volume 105. American Mathematical Society, Providence, RI, 2009.

[41] L. Li and B. Jafarpour. Effective solution of nonlinear subsurface flow inverse problems in sparse bases. *Inverse Problem*, 26(10), 2010.

[42] M.H. Loke and T. Dahlin. A comparison of the Gauss-Newton and quasi-Newton methods in resistivity imaging inversion. *Journal of Applied Geophysics*, 49(3):149–162, 2002.

[43] H. Maurer and J. Zowe. First and second-order necessary and sufficient optimality conditions for infinite-dimensional programming problems. *Mathematical Programming*, 16(1):98–110, 1979.

[44] D. McLaughlin and L.R. Townley. A reassessment of the groundwater inverse problem. *Water Resources Research*, 32(5):1131–1161, 1996.

[45] N.G. Meyers. An Lp-estimate for the gradient of solutions of second order elliptic divergence equations. *Annali Della Scuola Normale Superiore Di Pisa-Classe Di Scienze*, 17(3):189–206, 1963.

[46] N.G. Meyers and J. Serrin. H = W. *Proceedings of the National Academy of Sciences*, 51(6):1055–1056, 1964.

[47] E.D. Nezza, G. Palatucci, and E. Valdinoci. Hitchhiker's guide to the fractional Sobolev spaces. *Bulletin des Sciences Mathmatiques*, 2011.

[48] J. Nocedal and S. Wright. *Numerical Optimization, Second Edition*. Springer, New York, NY, 2006.

[49] S. Osher, M. Burger, D. Goldfarb, J. Xu, and W. Yin. An iterative regularization method for total variation-based image restoration. *Multiscale Modeling & Simulation*, 4(2):460–489, 2005.

[50] R.L. Parker. *Geophysical Inverse Theory*. Princeton University Press, Princeton, NJ, 1994.

[51] G. Pratt, C. Shin, and G.J. Hicks. Gauss-Newton and full Newton methods in frequency–space seismic waveform inversion. *Geophysical Journal International*, 133(2):341–362, 1998.

[52] L. Rondi and F. Santosa. Enhanced electrical impedance tomography via the Mumford–Shah functional. *ESAIM: Control, Optimisation and Calculus of Variations*, 6:517–538, 2001.

[53] E.M. Sevick-Muraca, J.P. Houston, and M. Gurfinkel. Fluorescence-enhanced, near infrared diagnostic imaging with contrast agents. *Current Opinion in Chemical Biology*, 6(5):642–650, 2002.

[54] E.M. Sevick-Muraca, E. Kuwana, A. Godavarty, J.P. Houston, A.B. Thompson, and R. Roy. Near infrared fluorescence imaging and spectroscopy in random media and tissues. *Biomedical Photonics Handbook*, pages 33–1, 2003.

[55] E.M. Stein. *Singular Integrals and Differentiability Properties of Functions*, volume 2. Princeton University Press, Princeton, NJ, 1970.

[56] A. Tarantola. *Inverse Problem Theory and Methods for Model Parameter Estimation*. SIAM, Philadelphia, PA, 2005.

[57] A.N. Tikhonov and V.Y. Arsenin. Solutions of ill-posed problems. *WH Winston*, 330:271, 1977.

[58] M. Webb. Analysis and approximation of a fractional differential equation. Master's thesis, Oxford University, Cambridge, UK, 2012.

[59] W. W-G Yeh. Review of parameter identification procedures in groundwater hydrology: The inverse problem. *Water Resources Research*, 22(2):95–108, 1986.

[60] K. Yosida. *Functional Analysis. Reprint of the Sixth (1980) Edition. Classics in Mathematics*, volume 11. Springer-Verlag, Berlin, 1995.